INFORMATION TO USERS

This manuscript has been reproduced from the microfilm master. UMI films the text directly from the original or copy submitted. Thus, some thesis and dissertation copies are in typewriter face, while others may be from any type of computer printer.

The quality of this reproduction is dependent upon the quality of the copy submitted. Broken or indistinct print, colored or poor quality illustrations and photographs, print bleedthrough, substandard margins, and improper alignment can adversely affect reproduction.

In the unlikely event that the author did not send UMI a complete manuscript and there are missing pages, these will be noted. Also, if unauthorized copyright material had to be removed, a note will indicate the deletion.

Oversize materials (e.g., maps, drawings, charts) are reproduced by sectioning the original, beginning at the upper left-hand corner and continuing from left to right in equal sections with small overlaps.

Photographs included in the original manuscript have been reproduced xerographically in this copy. Higher quality 6" x 9" black and white photographic prints are available for any photographs or illustrations appearing in this copy for an additional charge. Contact UMI directly to order.

Bell & Howell Information and Learning
300 North Zeeb Road, Ann Arbor, MI 48106-1346 USA
800-521-0600

POSTNATAL MATURATION OF THE ELECTRORETINOGRAM OF THE GUINEA PIG (*CAVIA PORCELLUS*)

Darren Behn
Department of Neurology and Neurosurgery
McGill University, Montréal
January 1999

A thesis submitted to the Faculty of Graduate Studies and Research in partial fulfillment of the requirements of the degree of Master of Science

ABSTRACT

Unlike most rodents, the guinea pig (*Cavia porcellus*) is born with its eyes open. It has been claimed that most of the functional and structural maturation of the retina takes place *in utero*. In fact, to our knowledge, no study has specifically examined if there was a postnatal maturation of the retina in guinea pigs. The aim of this study was to determine whether the retinal development of the guinea pig continued after birth. The results showed that both photopic (cone) and scotopic (rod) function continue to develop after birth, the former taking more time to reach maturity than the later.

RÉSUMÉ

Contrairement à la plupart des rongeurs, le cochon d'Inde (*Cavia porcellus*) naît avec les yeux ouverts. Des études antérieures ont suggéré que l'ensemble de la maturation structurelle et fonctionnelle de la rétine s'effectuait *in utero*. De fait, à notre connaissance, aucune étude n'a examiné s'il y avait une maturation postnatale de la rétine chez cette espèce animale. Le but de notre étude était donc de déterminer si le développement de la rétine du cochon d'Inde se poursuit après la naissance. Nos résultats montrent que tant la fonction photopique (cônes) que scotopique (bâtonnets) continuent de se développer après la naissance, la première prenant plus de temps à atteindre la maturité.

ACKOWLEDGMENTS

First and foremost, I would like to thank Dr. Pierre Lachapelle for his support, patience and encouragement over the past two years. His approach to science has shown me that the world of research is enjoyable and exciting, and not merely comprised of long hours of tedious work. He sets a professional and personal example that inspires one to go beyond his self-set limits. I have benefited from working with and learning from Dr. Lachapelle in many ways, all of which will contribute to my future academic and personal endeavors.

I would like to extend my sincere thanks and appreciation to Olga Dembinska for creating a stimulating atmosphere in the laboratory. I would also like to thank Eric Sémard for his expertise in animal care used in this research.

Of course, many thanks must go to my mother. She has always encouraged me to discover my potentials and pursue my abilities. Finally, I would like to thank Michelle for contributing to this thesis on a day-to-day basis in all the ways that are necessary yet invisible.

TABLE OF CONTENTS

ABSTRACT ii

RÉSUMÉ iii

ACKNOWLEDGEMENTS iv

LIST OF FIGURES viii

INTRODUCTION 1

The electroretinogram: definition and history 1

Retinal organization and histology 2

Components and origins of the ERG 6

The a-wave 6

The b-wave 9

The i-wave 10

The OPs 10

Characteristics of the ERG 12

The photopic hill: a feature of the cone ERG 13

Scotopic intensity response functions of the ERG 13

Light adaptation of the ERG 18

Dark adaptation of the ERG 18

Maturation of the ERG 19

Purpose 21

MATERIALS AND METHODS 23

Physiological recordings and data collection 23

Animal preparation 26

Recording procedure 27

Data analysis 29

RESULTS 33

Maturation of the photopic ERG 33

Amplitude parameters 33

Peak-time parameters 39

b-wave/a-wave parameters 39

Light adaptation effect 44

slow flicker parameters 47

Maturation of the scotopic ERG 53

Amplitude parameters 53

Peak-time parameters 63

b-wave/a-wave ratio 66

Dark adaptation parameters 69

A night blind guinea pig: an unexpected finding 72

DISCUSSION 76

Photopic responses 76

Photopic flicker responses 77

Interpreting the light adaptation effect 78

Scotopic responses 81

CONCLUSIONS 87

REFERENCES 89

LIST OF FIGURES

Figure 1	Organization of the retina	4
Figure 2	Typical ERG recorded from a human subject	8
Figure 3	Photopic intensity response function of the guinea pig	15
Figure 4	Scotopic ERG responses of the Spague-Dawley rat	17
Figure 5	Experimental set-up	25
Figure 6	A- A typical light adapted ERG B- A typical dark adapted ERG	32
Figure 7	Maturation of the photopic ERG	35
Figure 8	A- summary of the photopic a- and b-wave amplitudes B- summary of the photopic OP amplitudes	38
Figure 9	A-summary of the photopic a- and b-wave peak-times B- summary of the photopic OPs peak-time	41
Figure 10	Photopic b/a-wave ratio	43
Figure 11	A- Light adaptation effect ERG tracings at age P_1 B- Light adaptation effect ERG tracings at age P_{75} C- The b-wave amplitude for 20 min of light adaptation	46
Figure 12	A- OPs evoked to a flicker presentation at age P_{1-2} B- OPs evoked to a flicker presentation at age P_{75}	49
Figure 13	Effect of a flicker presentation at ages P_{1-2} and P_{75}	51
Figure 14	Maturation scotopic intensity response functions	54

Figure 15	Maturation of the scotopic ERG and OPs	57
Figure 16	Summary of intensity-responses of the scotopic ERG	59
Figure 17	A- Summary of the scotopic a- and b-wave amplitudes B- Summary of the scotopic OP amplitudes	62
Figure 18	A- Summary of the scotopic a- and b-wave peak-times B- Summary of the scotopic OPs peak-time	65
Figure 19	Maturation of the scotopic b-wave/a-wave ratio	68
Figure 20	A- ERG tracings of the 1st minute of dark adaptation B- Intensity-response of the 1st minute of dark adaptation	71
Figure 21	A- Scotopic ERG tracings of a night blind guinea pig B- Photopic ERG tracing of a night blind guinea pig C- Scotopic response curve of a night blind guinea pig	74

INTRODUCTION

The electroretinogram: definition and history

In response to a light stimulus, the retina generates a bipotential known as the *electroretinogram* (ERG) which can be captured at the corneal surface of the eye. Although first identified by Holgrem in 1865, it was Dewar who demonstrated, in 1877, that a light stimulus could produce an electric potential between a corneal and optic nerve electrode. As a result of these early experiments, the ERG is considered to be the first biopotential recorded from humans.

In 1933, Granit distinguished three separate components of the ERG, namely P-I, P-II, and P-III, using the dark adapted, rod-dominated cat retina. The Roman numerals specified the order in which a progressive increase in ether narcosis suppressed the various ERG components in the cat. This was the first study to demonstrate that the ERG response reflected the complex activity of more than one retinal generator. Further work led scientists to rename the P-I, P-II, and P-III processes by which the components of the ERG are now conventionally named. The initial negative deflection known as P-I was renamed as the a-wave, the positive wave known as P-II was designated as the b-wave, and the slow positive P-III potential was termed the c-wave. Subsequently, the P-III

component was found to consist of two separate components: 1) the initial phase which reflects the activity of the photoreceptor cells (the leading edge of the a-wave); and 2) the slow developing phase, which likely originates in the Müller cells (Granit, 1962; Tomita, 1963; Brindley, 1957).

The use of the ERG for the purpose of analyzing and diagnosing human pathologies was greatly expanded with the development of non-invasive contact lens electrodes (Karpe, 1945; Henkes, 1951; Burian and Allen, 1954). In 1945, Karpe was the first researcher to clinically utilize the ERG as a diagnostic tool. He discovered a correlation between an extinguished ERG and the early signs of the human condition: *Retinitis Pigmentosa* (RP).

Advancements in computer technology helped to overcome many of the problems inherently associated with recording electrical signals. For example, by adding the responses obtained from repetitive stimuli, computer averaging allowed the extraction of the evoked biopotential from electrical noise and later allowed vast amounts of data to be easily stored and retrieved. Use of the microelectrode also helped to identify more clearly the origins of the ERG components within the retina (Tomita and Torihama, 1956; Brown and Wiesel, 1961a,b). However, the more advanced electronic recording methods also revealed the complexity of the ERG. As a result, the origin of many of the ERG components still remains unclear.

Retinal organization and histology

As shown in figure 1 and as reviewed by Dowling (1970), the vertebrate retinal architecture consists of several different cells; all of which contribute to the process of

Figure 1

The major cell types and neuronal organization found in the vertebrate retina. A: amacrine. B: bipolar, C: cone, G: ganglion cell, H: horizontal cell, INL: inner nuclear layer, IPL: inner plexiform layer, IS: inner segment, OS: outer segment, ONL: outer nuclear layer, OPL: outer plexiform layer, PL: photoreceptor layer, R: rod (adapted from Dowling and Boycott, 1966).

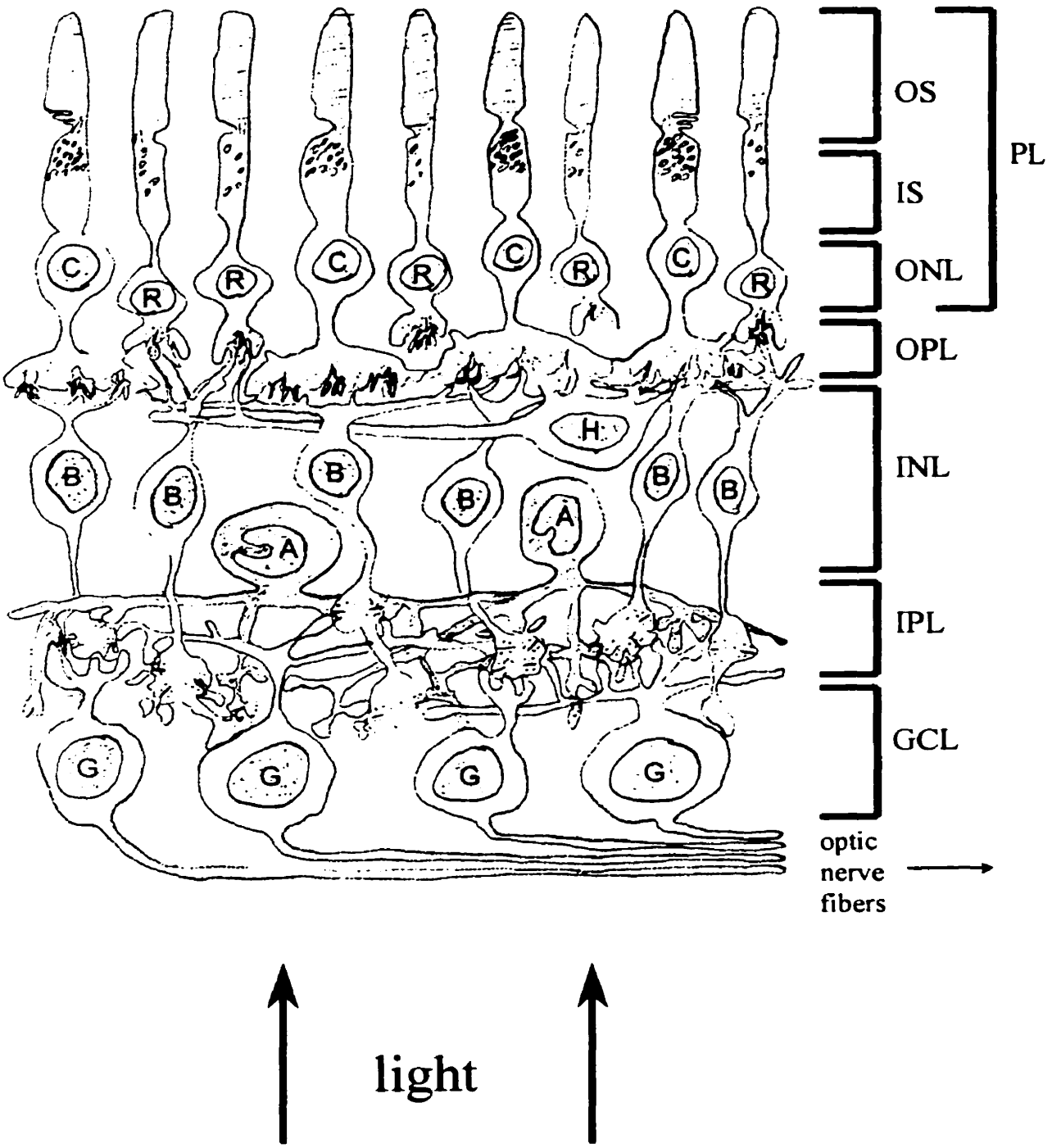
C
R
B
A
H
G
OS
IS
ONL
PL
OPL
INL
IPL
GCL
optic
nerve
fibers
light

transferring light information from the photoreceptors inwardly to the retinal ganglion cells and ultimately the visual cortex.

The *photoreceptor layer* contains the photoreceptor's *outer segment* which houses the retina's light sensitive molecules, such as the rod's rhodopsin. The *outer nuclear layer* is formed from the photoreceptor's cellular bodies. Information encoded as an electrical potential is transmitted from the photoreceptors to the bipolar cells which align to form the outer nuclear layer. The synapses between the photoreceptors and the bipolar cells are essential for communication. These synapses construct a distinctive layer referred to as the *outer plexiform layer.*

The *inner nuclear layer* contains a number of cellular bodies which participate in either signal transmission or in signal modification. While the signal transmission cells are believed to be ON/OFF bipolar cells and glial cells (referred to as Müller cells in the retina), the cells involved with signal modification are thought to be horizontal, amacrine, and interplexiform cells. The output of these cellular bodies project to the retinal ganglion cells that form the ganglion cell layer. The synaptic connections, which separate the inner nuclear layer from the ganglion cell layer, are referred to as the *inner-plexiform layer*. The axons of the ganglion cells travel across the retina to a central point named the *optic nerve head* where they merge to form the *optic nerve* which exits the eye, carrying visual information to the brains' visual centers.

Components and origins of the ERG

The ERG is an evoked potential with a waveform that can be broken down into distinctive components. Typically, the ERG morphology is characterized by an initial negative deflection referred to as the a-wave, followed by a larger positive potential known as the b-wave (figure 2-A). An interesting feature of the b-wave is the smaller wavelets which appear to "ride" on its ascending lope. These wavelets are usually referred to as the oscillatory potentials (OPs) and can be isolated by changing the recording bandwidth from 1-1000Hz to a narrower bandwidth of 100-1000 Hz (figure 2-B).

The a-wave

The a-wave is the first distinctive portion of the ERG and is presumed to originate at the level of the photoreceptors. Photoreceptors absorb light within their outer segments causing the photoreceptor pigment to become excited. When the photoreceptor pigment reaches an excited state, it initiates a sequence of molecular event which eventually leads to a hyperpolarization. This electrical response has long been associated with the initial negative deflection or the a-wave of the ERG (Brown, 1968, Penn and Hagins, 1969; Heynen and Van Norren, 1985). Recent computational models have advanced the above theory by demonstrating a quantitative relationship between the leading edge of the a-wave and electrical activity of the photoreceptors (Hood and Birch, 1990a,b; 1993; 1995). However, Bush and Seiving (1994) challenged this widely accepted view and claimed that, in some conditions, there is a significant contribution of second order hyperpolarizing cells to the genesis of the a-wave.

Figure 2

A typical light adapted (background: 30 cd.m^{-2}) ERG (tracing A, 1-1000Hz bandwidth) and OPs (tracing B, 100-1000 Hz bandwidth) simultaneously recorded from a normal subject to a flash intensity of 0.9 log cd. m^{-2} sec. Vertical arrows indicate flash onset. Tracings represent averages of 20 flashes presented at interstimulus intervals of 1.028 sec. Calibration: horizontal: 20 msec; vertical: 25 μV (tracing A), 5 μV (tracing B).

A

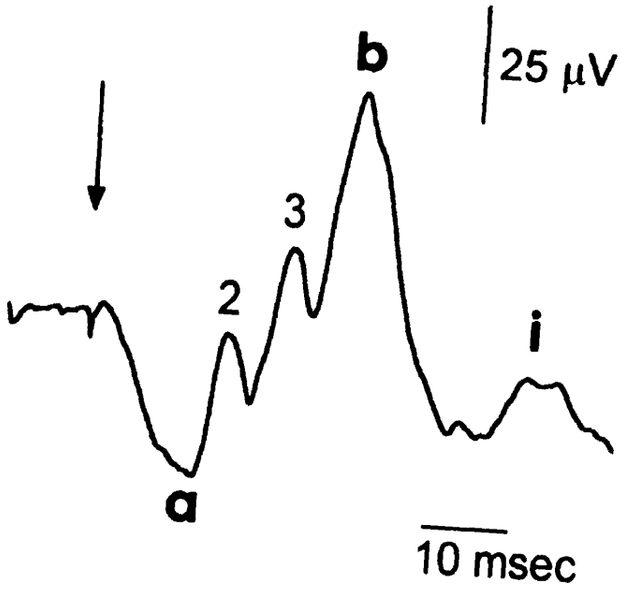

B

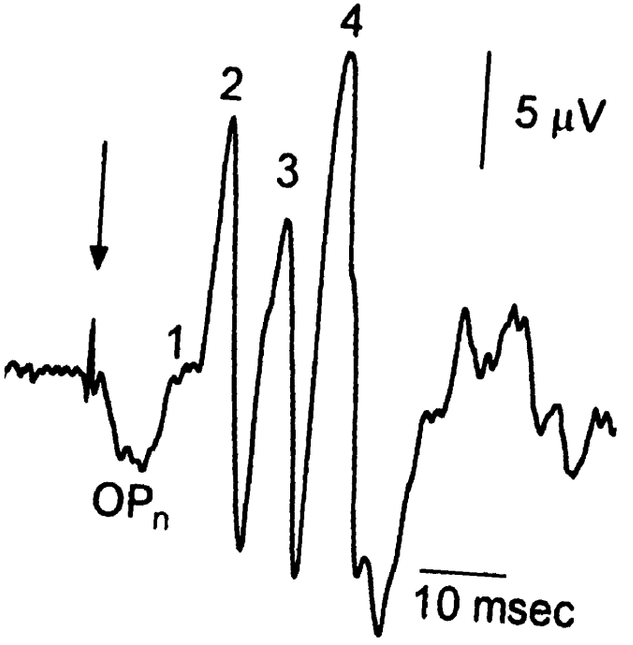

The b-wave

The b-wave is the most prominent component of the ERG. Although it has been studied extensively, its origin has not been fully determined. Of the three retinal nuclear layers (photoreceptors, second-order neurons, and ganglion cells) likely to be at the origin of the b-wave, the photoreceptors (Brown, 1968) and the ganglion cells (Noell, 1954) were eliminated as probable locations. This left second-order neurons as the most probable location responsible for the b-wave generation. Intra-retinal recordings further support this view given that the b-wave was shown to reach its highest amplitudes at the inner nuclear layer (Brown and Wiesel, 1961a,b).

There are two types of bipolar cells which can be distinguished as being either depolarized (ON) or hyperpolarized (OFF) by the light stimulus. The consequence of activating a depolarizing ON-bipolar cell results in an increase in extracellular potassium, primarily within the postreceptoral outer plexiform layer. Miller and Dowling (1970) postulated that the b-wave is produced from Müller cells which depolarizes in response to an increase of extracellular K^+ resulting from a light induced depolarization of the second order neurons. The b-wave would be recorded from the radial flow of current moving through the retina resulting from the Müller cell's depolarization.

Although this model of b-wave genesis has received substantial support from a number of studies (Dick and Miller, 1978; Newman, 1980; Newman and Odette, 1984), a more recent theory suggests that the bipolar cells interact in a "push/pull" manner to produce the b-wave (Sieving et al., 1994). Sieving theorized that the depolarizing bipolar cells are responsible for the initial "push" of the ascending part of the b-wave, while the hyperpolarizing cells and the Müller cells compete to sink the K^+ expelled by the

depolarizing ON-bipolar cells and limit or "pull" the b-wave magnitude back down. Both theories gained support from the demonstration that the glutamate analog, 2-amino-4-phosphonobutyric acid (APB), which eliminates the response of ON-bipolar cells, abolishes the b-wave from ERG recordings (Stockton and Slaughter, 1989; Tian and Slaughter, 1994; Hanitzsch et al., 1996, Guite et al., 1990).

Xu and Karwoski (1994; 1996) further claimed that the b-wave is generated directly by the bipolar cells and not from Müller cells after they showed that the pharmacological removal of the buffer currents of Müller cells (using Ba^{-}) do not eliminate the b-wave potential. Although these findings clearly support the concept that bipolar cells are the source of b-wave genesis, further investigations are warranted to substantiate this claim.

The i-wave

Nagata (1963) identified the i-wave as a post-b-wave ERG component that reflects an OFF-response to ERGs evoked to brief flashes of light. Although very few studies have investigated the origin of this ERG component, a study from our group (Rousseau et al, 1996) suggests that the i-wave is generated at the level of the retinal ganglion cells.

The OPs

The most intriguing components of the ERG are the small wavelets seen on the ascending limb of the b-wave which are referred to as oscillatory potentials (OPs) (Cobb and Morton, 1954). Although much work has focussed on the exact origin of the OPs, the genesis of these components remain unclear. However, several studies have helped to

narrow the general area from which the OPs originate. Studies utilizing intraretinal recording techniques have determined the inner retinal layer and/or the inner plexiform layer as the most probable sites from which the OPs originate (Brindley 1956; Yonemura and Hatta, 1966; Ogden, 1973; Wachtmeister and Dowling, 1978; Heynen and van Norren, 1985; Heynen et al., 1985; Yanagida et al., 1988). Depth profile studies have also helped to eliminate horizontal cells as the cellular structure responsible for OP genesis (Ogden, 1973). Further investigations have ruled out the photoreceptors, retinal ganglion cells, and Müller cells as the primary site for OP generation (Brown, 1968; Miller and Dowling, 1970; Ogden, 1973). Specifically, intraretinal recordings from the mudpuppy excluded Müller cells because they did not produce an OP-like response (Miller and Dowling, 1970). Following an occlusion of the central retinal artery, the OPs and the b-wave were eliminated while the a-wave (photoreceptors) remained unaffected (Brown, 1968). Finally, OPs remained normal following tetrodotoxin treatment which is known to block the discharge of the retinal ganglion cells (Ogden, 1973).

Many investigators have examined the relationship of the b-wave to the presence or absence of the OPs. Lachapelle et al., (1983) noted that the ERG amplitude in patients afflicted with *Congenital Stationary Night Blind* (CSNB) was decreased proportionally to the absence of two OPs. Furthermore, Gorfinkel et al., (1988) examined the development of the ERG and OPs in the neonatal rabbit and reported that changes in peak time and amplitude of the photopic b-wave are consistent with the development of new components corresponding to the OPs. This study supports a theory that postulates that the OPs might be the building blocks of the b-wave (Lachapelle et al., 1983; Lachapelle and Molotchnikoff, 1986a; Gorfinkel and Lachapelle, 1990).

However, others have proposed an alternate theory indicating separate processes for the b-wave and the OPs. This stems from observations that OPs can be selectively abolished as seen in patients with diabetic retinopathy (Yonemura et al., 1962; Brunette and Desrochers, 1970; Speros and Price, 1981). This theory is also supported by ERG developmental studies in the cat (Hamasaki and Maguire, 1985) which demonstrated that the formation of the a-wave precedes the formation of the b-wave and the b-wave precedes the formation of the OPs. Differential maturation of the ERG components is also noted in the albino rabbit where the OPs and a-wave appear at day eight, whereas the b-wave appeared at day 10 (Noell, 1958). If the OPs are the building blocks of the b-wave, it would be expected that the OPs and the b-wave would develop in unison. Understanding the role of the OPs remains a fundamental question of retinal electrophysiology.

Characteristics of the ERG

The ERG response can be evoked under a variety of conditions, each of which can produce a distinctive ERG. The dark adapted rod ERG also known as the scotopic ERG is the electrical response recorded from the rod system when evoked to a light stimulus after the retina has been dark adapted for a minimum period of time (usually at least 20 minutes). Similarly, the light adapted cone ERG also known as the photopic ERG is the electrical response recorded from the cones system following a period in which the retina was light adapted to a constant background (30 cd. m^{-2}) for at least 10 minutes. The evoked response of the ERG can also be distinguished during different stages of retinal development and/or under different illuminating conditions.

The photopic hill: a feature of the cone ERG

An intensity response function can be constructed from ERGs evoked to a range of stimulus intensities. The light adapted intensity response function for humans typically displays an increase in the a-wave and b-wave amplitudes as the stimulus intensity is increased until a peak amplitude (V_{max}) is reached (Peachey et al., 1989b; Wali and Leguire, 1992). Unlike the a-wave amplitude which continues to increase in amplitude with an increase in stimulus intensity, further increases to the stimulus intensity beyond V_{max} evokes a b-wave response of smaller amplitude. This phenomenon has been named the photopic hill (Wali and Leguire, 1992). Similar to that reported in humans, a typical photopic intensity response function obtained from the guinea pig is presented at figure 3 where the peak amplitude of the b-wave is evoked to a flash intensity of 0.9 log $cd.m^{-2}sec$. The V_{max} of the photopic hill is thought to represent the optimum response of the b-wave generators (Wali and Leguire, 1992).

Scotopic intensity response functions of the ERG

As shown at figure 4 for the Sprague-Dawley rat, the scotopic intensity response function for of most animals, including humans, displays an increase in the b-wave amplitude as the stimulus intensity is increased from dim intensities until it reaches a plateau or the first V_{max} (Peachey, 1989a). Unlike the light adapted cone ERG intensity response curve which exhibits a decrease in amplitude beyond the V_{max} (figure 3), the dark adapted rod ERG intensity response curve plateaus and then increases again constituting a second limb (Peachey et al., 1989a). This second limb does not result from interactions between rod and cone system signals as was suggested by Schneider et al. (1986), but

Figure 3

Representative light adapted (30 $cd.m^{-2}$) ERGs (1-1000 Hz bandwidth) obtained from a guinea pig (A) were recorded to flashes of white light of increasing flash intensity spanning over a 1.5-log unit range with a maximum flash intensity of 1.2. log $cd.m^{-2}$ sec. Light adapted intensity-response function for the b-wave amplitude is shown in B. The b-wave reached a maximum amplitude when evoked to a flash intensity of 0.9 log $cd.m^{-2}$ sec. Each data point represents the mean ± SEM of measurements obtained from 8 guinea pigs. Calibration: horizontal: 20 msec (A); vertical 100 μV (A).

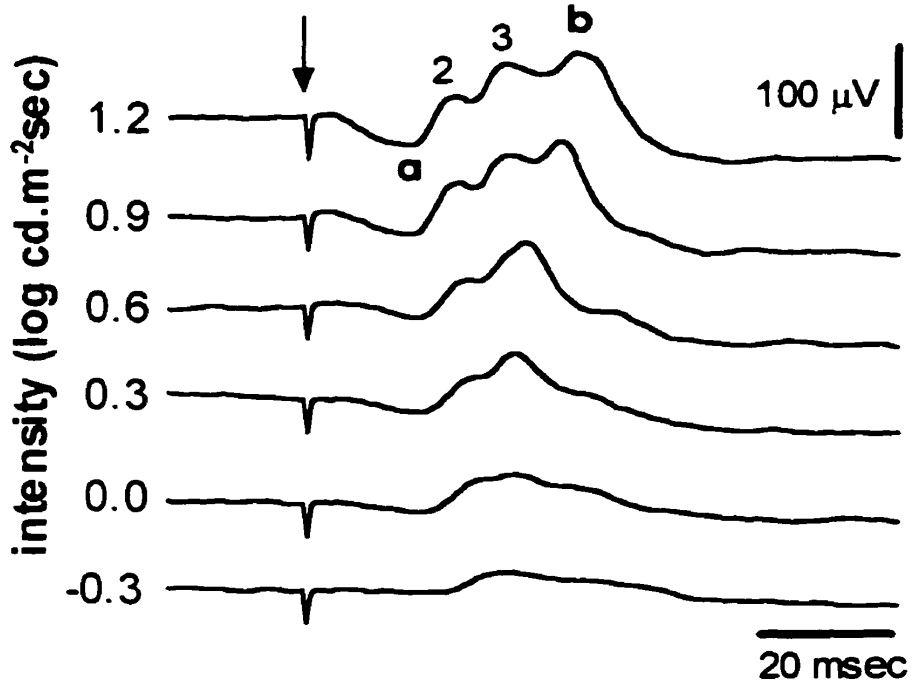
b
3
2
a
100 µV
1.2
0.9
0.6
0.3
0.0
-0.3
intensity (log cd.m-2sec)
20 msec

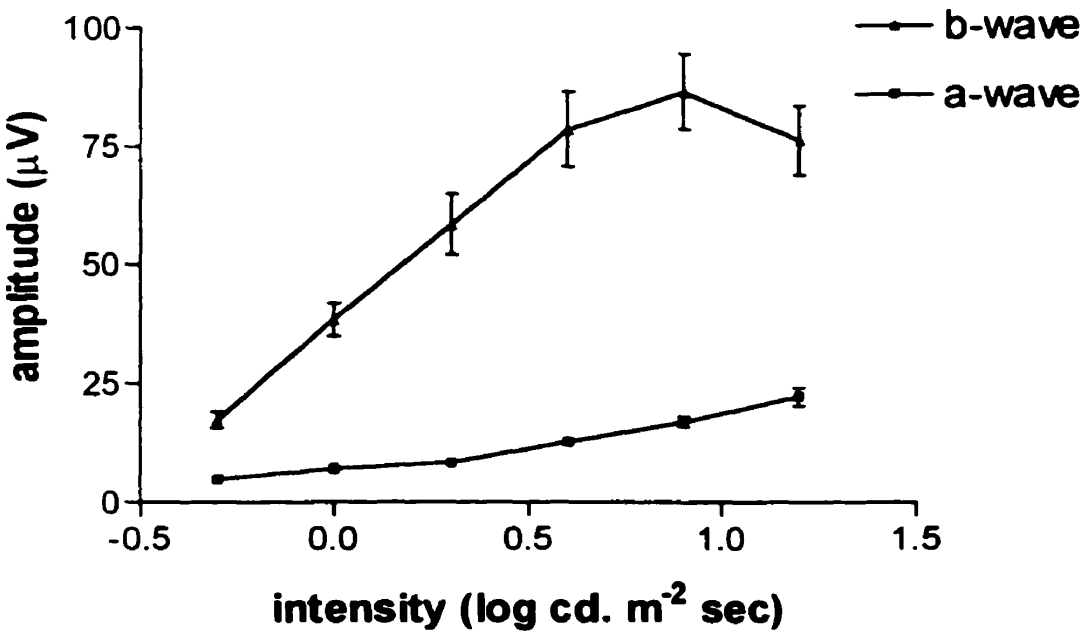
b-wave
a-wave
100
75
50
25
0
amplitude (µV)
-0.5
0.0
0.5
1.0
1.5
intensity (log cd. m-2 sec)

Figure 4

Representative dark adapted ERG recordings (A) obtained from a Sprague-Dawley rat evoked to flashes of white light spanning over a 6 log unit range (-5.1 to 0.9 log cd.m^{-2}sec). Each ERG tracing represents an average between 2 and 5 responses depending on the stimulus intensity. Vertical arrows identify flash onset. Graphic representation of the intensity-response function obtained from a dark adapted Sprague-Dawley rat is shown in B. Calibration: horizontal: 20 msec (A); vertical 300 μV (A).

A

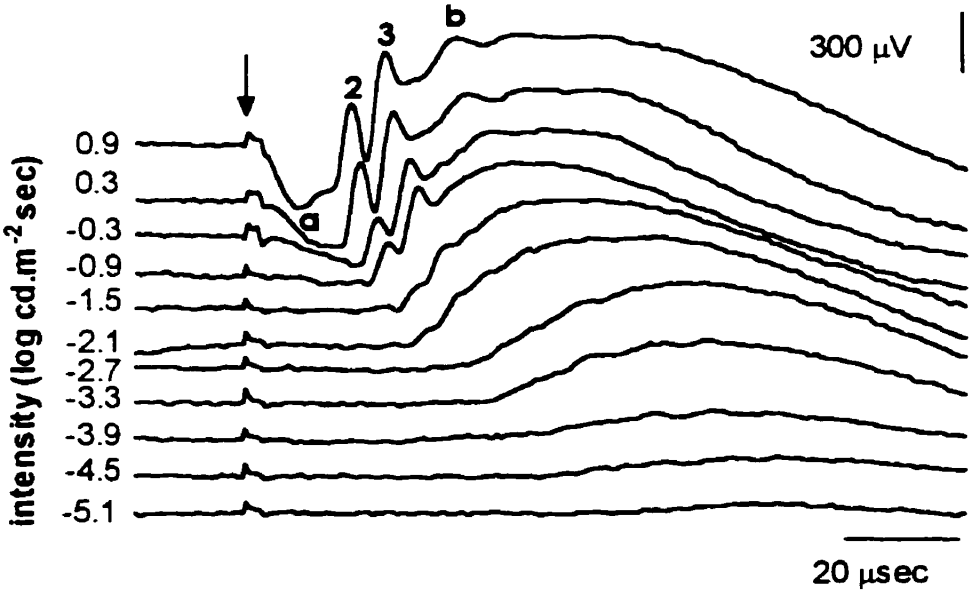
300 µV
a
b
1
2
3
0.9
0.3
-0.3
-0.9
-1.5
-2.1
-2.7
-3.3
-3.9
-4.5
-5.1
intensity (log cd.m-2sec)
20 µsec

B

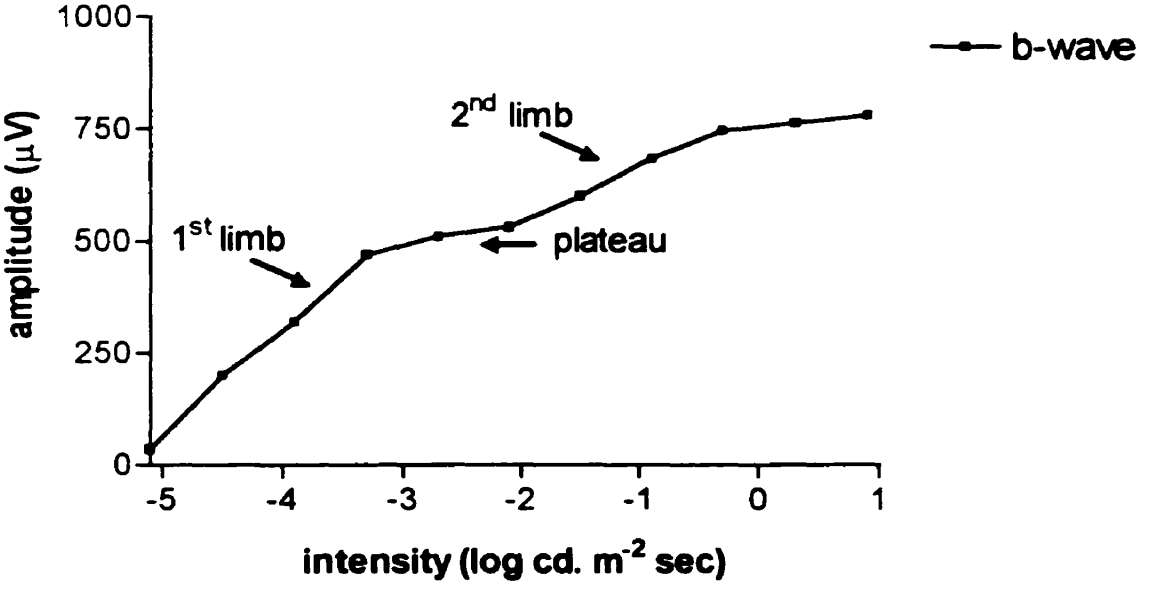
b-wave
1000
750
500
250
0
amplitude (µV)
2nd limb
1st limb
plateau
-5
-4
-3
-2
-1
0
1
intensity (log cd. m-2 sec)

thought to be determined by an intensity-dependent algebraic summation of the components that comprise the rod system (Peachey et al., 1989a).

Light adaptation and the ERG

In most mammals, it is well known that upon light onset, following an ample period of dark adaptation, the timing of the cone ERG shortens and/or its amplitude increases with increasing light exposure time (Burian 1954, 1981; Armington and Biersdorf, 1958; Lachapelle, 1987; Miyake et al., 1987; Gouras and Mac Kay, 1989; Peachey et al., 1989b; Koichiro and Sieving, 1992). Moreover, in humans this effect becomes more pronounced with at least a 10 minute period of dark adaptation (Miyake et al., 1988; Benoit and Lachapelle, 1995). This phenomenon is referred to as the light adaptation effect (LAE). Although the mechanism underlying this phenomenom has not been identified, various explanations have been advanced. Armington and Biersdorf (1958) suggested the possibility that a change in the standing potential of the eye might be involved, while Gouras and Mackay (1989) more recently suggested that the reason for this effect was the re-depolarization of the cone photoreceptors during light adaptation.

Dark adaptation and the ERG

Similarly, the magnitude of scotopic ERGs grow with progressive dark adaptation. The regeneration of the rhodopsin photopigment, which is inactive in light adapted conditions, is considered responsible for this response (DeMolfelta et al., 1968; Brunette, 1969; Wachtmeister, 1973; Lachapelle et al., 1990). Differences found between the initial phase (the first minute of dark adaptation) and the fully dark adapted phase emphasize the

contribution of the rod system to the genesis of the scotopic ERG (King-Smith et al., 1986; Lachapelle et al., 1990). The primary mechanism underlying this response has been suggested to be the adaptation within the outer segments of the rod photoreceptor to a dark environment. The rod photoreceptor becomes more sensitive due to the regeneration of rhodopsin and the scotopic b-wave subsequently increases in amplitude (Brunette, 1969).

Maturation of the ERG

The ERG has been used for assessing the developmental status of the visual system in animals models such as the cat (Hamasaki and Maguire, 1985; Ikeda and Jacobson, 1982), the dog (Gum et al., 1973; Kirk and Boyer, 1973), the rat (Braekevelt and Hollenberg, 1970; Kurihara, 1977; el Azazi and Wachtmeister, 1990,1991), and the rabbit (Sanada, 1962; Gorfinkel et al., 1988, Gorfinkel and Lachapelle, 1990). Most animal models possess a visual system that is immature at birth. For example, Hamaski and Maguire (1985) concluded that the postnatal development of the kitten's retina occurs in three distinct stages: 1) the first stage is characterized by the initial appearance of ERG components concurrent with the development of the outer segment of the photoreceptor; 2) the second stage is characterized by a rapid amplitude increase of the ERG components and the appearance of adult-like retinal cell layers; 3) the third and final stage of retinal development is characterized by a slow differentiation phase which can take several months.

In humans, most neural differentiation and synaptic establishment occurs *in utero* (Winkelman and Horsten, 1962; Shipley and Anton, 1964). Whether animals that share

this precocial characteristic with humans generally undergo the same three stages of retinal development as animals with an immature retinal system at birth is a scientific question that remains unanswered.

Purpose

Most studies which examined the maturation of the ERG have done so using an animal model born with an extremely immature retina (Hamasaki and Maguire, 1985; Ikeda and Jacobson, 1982; Gum et al., 1973; Kirk and Boyer, 1973; Braekevelt and Hollenberg, 1970; Kurihara, 1977; Gorfinkel et al., 1988; Sanada, 1962). These animals, are born with their eyes closed; the opening of the eye (approximately 8-14 days after birth) usually corresponds to the initial recording of an ERG. Previous investigations have identified 3 stages to the maturational process of the retina as evaluated by the ERG: 1) an initial phase; 2) a rapid phase; and, 3) a slow differentiation phase.

Unlike most rodents, the guinea pig is born with its eyes open and an adult-like retina (Bornschein, 1959; Van Hof and Usami, 1967; Legein and Van Hof, 1970; Huang et al., 1990). Although none of these studies have specifically investigated the postnatal maturation of the retina, Huang et al. (1990) identified two stages of retinal maturation both taking place *in utero*: 1) the initial development of ERG components occuring between the 55^{th} and 64^{th} day of gestation (full term is 68-69 days); and, 2) final maturation to an adult-like ERG between the 64^{th} day and birth.

The purpose of this study was to determine whether the retinal development of the guinea pig continues after birth (i.e. a third differentiation stage), or if retinal development is already complete at birth. If retinal development does continue after birth, it must be determined which components of the ERG reflect development. More specifically, the development of the photopic and scotopic ERG will be examined, paying close attention to the a-wave, b-wave, and OP components. Furthermore, it will be investigated if the process of light adaptation is modified with retinal development.

The knowledge gathered from developmental differences in an animal model born with an adult-like retina and ERG will help to refine the investigative techniques used and clarify the maturation of retinal function in other models born with a near mature retina, such as, the human infant (Zetterström, 1951; Barnet et al., 1965; Breton et al., 1995; Mets et al., 1995).

MATERIALS AND METHODS

Physiological recordings and data collection

The experimental set-up is schematically shovn in figure 5. Two Grass P-511K analog preamplifiers (Grass Instruments, Quincy, MA, USA), were used to record the evoked biopotential from the retina. The first amplifier was used to record the conventional ERG. Its bandwidth was set between 1 and 1000 Hz (Tsuchida et al., 1973) and amplified the signal 10 000 times. The second amplifier was set to selectively record the oscillatory potentials by setting the bandpass between 100 and 1000 Hz (Tsuchida et al., 1973) and amplifying the evoked potential 50 000 times. The outputs from the preamplifiers were averaged and stored using the Biopac MP100 Acknowledge System (BIOPAC Sytems Inc., Goleta, CA) and displayed on a computer monitor and oscilloscope. The acquisition period was set at 250 msec with 5 data points/msec and a delay of 20 msec was set before the flash onset to establish a baseline response. Each recorded response was stored on diskettes for further analysis and measurements.

Figure 5

Experimental set-up. Biopotenitals were evoked to flashes of white light delivered by a photostimulator. The signals were amplified 10 000 times (1-1000 Hz conventional ERG) and 50 000 times (100-1000 Hz specific OP recordings) by two separate preamplifiers. An oscilloscope permitted the visualization of the amplified signal. The amplified analog signal was converted into a digital signal and responses were averaged using a computer. The averaged ERG and OPs were stored on diskette and printed on paper for further analysis.

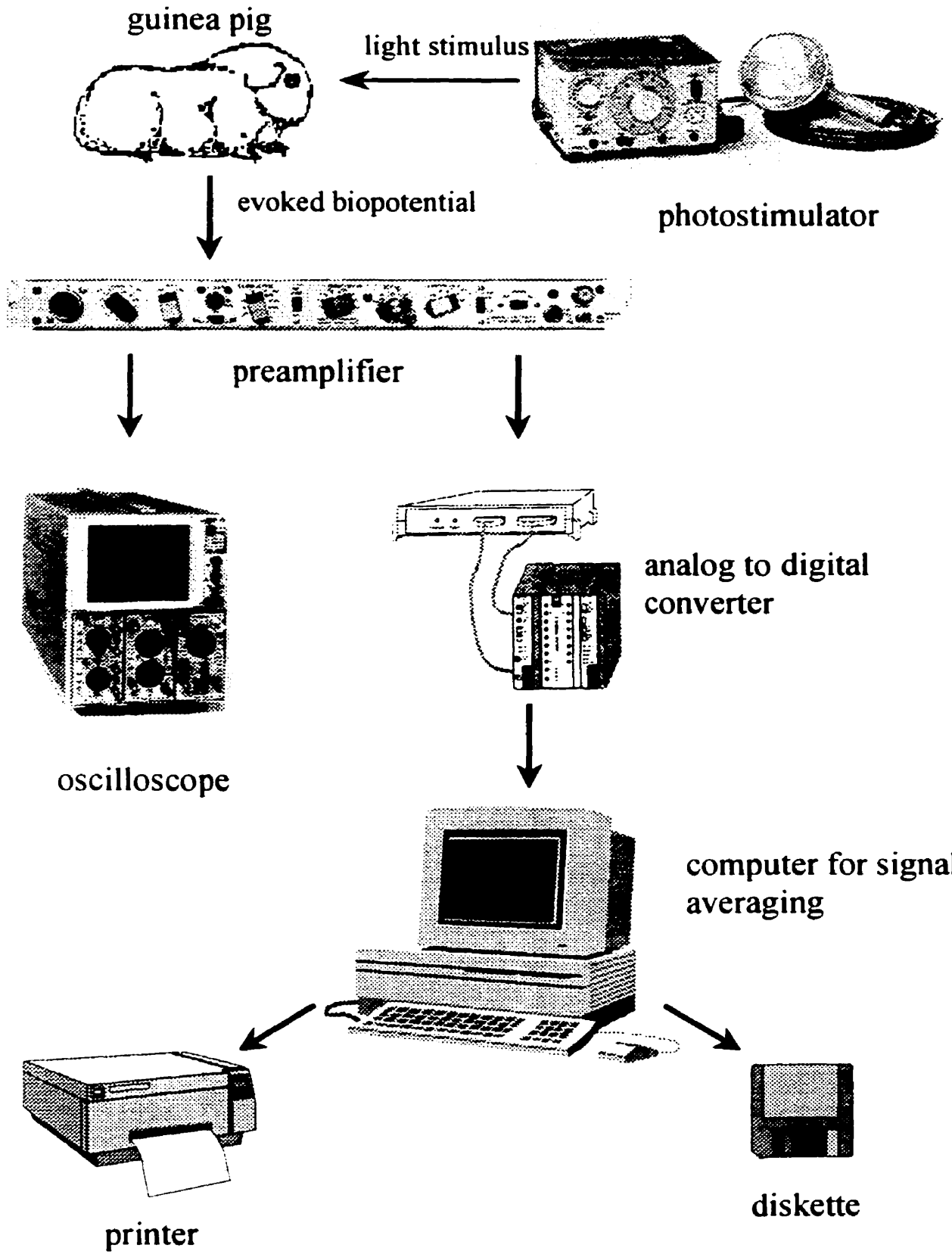
guinea pig
light stimulus
evoked biopotential
photostimulator
preamplifier
analog to digital converter
oscilloscope
computer for signal averaging
printer
diskette

Animal preparation

A total of 29 Hartley Guinea Pigs (Charles River, St-Constant, Québec) were used in this study according to a protocol approved by the McGill University-Montréal Children's Hospital Animal Care Committee. To evaluate the photopic hill, 8 adult guinea pigs were used. The remaining 21 guinea pigs were used to evaluate the maturation of the photopic and scotopic ERGs/OPs determined by the recording procedures listed below. Four of the 21 guinea pigs died within the first 10 days of life. Guinea pigs were housed in our animal care facility equipped with an automated, 12 hour light/dark environment. Depending on the position of the cage relative to the ceiling lights, the illumination inside the cages was maintained between 20-30 $cd.m^{-2}$. This intensity was far below the light intensity shown to produce retinal degeneration in the albino animals (Semple-Rowland and Dawson, 1987).

Pregnant guinea pigs were closely monitored one week prior to the expected delivery date. Immediately following delivery (P_1), neonatal guinea pigs were weighed, their eyes inspected to confirm that they were open, and prepared for experimentation. Measurements were obtained every second or third day (depending on the litter) for 5 weeks and then once a week until ages P_{75}.

Prior to ERG measurements, guinea pigs were anaesthetized with an intra-muscular injection of a ketamine (85 mg/kg) and zylazine (5 mg/kg), a mixture known to have no notable effect on ERG amplitudes compared to inhalation anesthetics (van Norren and Padmos, 1975). The pupil was dilated with two drops of 1% cyclopentolate hydrochloride, after which the guinea pig was placed in a ganzfeld-like chamber of our design. A DTL (27/7 X-Static® silver coated conductive nylon yarn: Sauquoiot Industries,

Scranton, Pa, USA) electrode (Dawson et al., 1979; Lachapelle et al., 1993; Hébert et al., 1996) was placed on the corneal surface which was kept moist with two drops of 1-% methylcellulose. A reference electrode (Grass E5 disc electrode, Grass Instruments, Quincy, MA, USA) was placed in the mouth and a ground electrode (Grass E2 subdermal electrode, Grass Instruments, Quincy, MA, USA) was inserted into the mid-dorsal skin.

Recording procedure

Scotopic ERGs

Dark adapted, ERG and OP responses were obtained following a 12 hour period of dark adaptation to maximize the rod response. Scotopic (dark adapted) intensity response functions were generated with flashes of white light (Grass PS 22 Photostimulator, 20 msec in duration, Grass Instruments, Quincy, MA, USA), spanning over a 6 log unit range with a maximal intensity of 0.9 log $cd.m^{-2}$ sec in energy. Progression of the flash intensity was made in 0.3 log unit increments. For this protocol each response represents an average of 2-5 flashes depending on the stimulus intensity. To avoid the conditioning flash effect previously reported to affect dark-adapted ERGs, a minimum inter-stimulus period of 10 seconds was maintained for all scotopic recordings (Lachapelle et al., 1990; Peachey et al., 1987).

First minute of dark-adaptation

Scotopic ERGs and OPs were also obtained within the first minute of dark-adaptation. For this procedure, all guinea pigs were light adapted to a full-field background illumination of 30 $cd.m^{-2}$ for at least 5 minutes. Following this period of light

adaptation, the background lights were turned off and averages of ERGs and OPs were immediately obtained for one stimulus intensity. To generate the scotopic intensity response functions, the same stimulus intensities as described above were used. All responses for this procedure represent an average of 5 flashes.

Photopic ERGs

Light adapted, cone-mediated, ERGs and OPs were obtained following the recording of the scotopic responses described above and following a light adaptation period of at least 20 minutes to ensure a maximal cone response and to avoid any light adaptation effect phenomenon (Lachapelle et al., 1987; Peachey et al., 1990). A diffusing screen fitted with miniature halogen lamps was placed between the flash stimulator unit and the guinea pig to provide a full-field background illumination of 30 $cd.m^{-2}$. Light adapted ERGs were evoked to flashes of white light 0.9 log $cd.m^{-2}$ sec (Grass PS 22 Photostimulator, 20 μsec in duration, Grass Instruments, Quincy, MA,USA) and averages of 20 responses were obtained (inter-stimulus interval of 1.024 seconds). These photopic parameters were previously shown to yield an isolated cone response from rodents (Peachey et al., 1993).

The light adaptation effect

To evaluate the light adaptation effect (LAE), photopic ERGs were recorded at light onset (t_0), immediately after a 12-hour period of dark adaptation, and at five-minute intervals for twenty minutes (i.e. t_5, t_{10}, t_{15} and t_{20}). The same photopic parameters

described above were used to generate the photopic responses that represent an average of 5 flashes at each time interval.

Slow flicker stimulus

Maturation of the photopic function was also investigated with a flickering stimulus as it was previously shown that each photopic OP was differentially affected by this form of stimulus (Lachapelle, 1991). Photopic ERG/OP responses were also obtained using a slow flicker stimulus. As stated above for photopic conditions, all guinea pigs were light adapted to a full-field background illumination of 30 $cd.m^{-2}$ for at least 20 minutes. As determined with an interval generator unit (Grass S10 VSA Stimulator, Grass Instruments, Quincy, MA, USA), a flash stimulus of 0.9 log $cd.m^{-2}$ sec in energy was used at the following six rates of presentation to evoke the OP responses: 0.5Hz, 1Hz, 2Hz, 4Hz, 8Hz, and 16 Hz. Each response represents an average of 50 flashes.

Data analysis

Data analysis consisted of measuring the amplitudes of the ERG components according to a method previously described (Lachapelle, 1987). The left tracings of figure 6-A and 6-B shows photopic and scotopic ERG recordings (1-1000 Hz bandwidth) obtained from an adult Guinea Pig and identifies the different ERG components. The amplitude of the a-wave was measured from baseline at flash onset (indicated by the arrow) to the first most negative trough. The b-wave amplitude was measured from the a-wave tough to the next most positive peak (the b-wave). The a- and b-wave peak times

were measured from flash onset to the a-wave trough and the peak of the b-wave, respectively.

The right tracings of figure 6-A and 6-B illustrate the more selective amplification of the OPs (100-1000Hz bandwidth). The first negative trough is usually identified "OP_n". Its amplitude was measured from baseline to trough. The amplitude of the next OP, referred to as OP_1, was measured from trough to peak. Like in human responses, the guinea pig OP_1 is an oscillatory potential which is best evidenced following a bright flash stimulus (Lachapelle and Molotchnikoff, 1986a). Although small, the trough immediately following OP_1 is used to measure the amplitude of OP_2. Similarly, the amplitudes of the remaining OPs were measured from preceding trough to peak. As shown in the left tracing of figure 6-A and in the remainder of the text, waves 2 and 3 will refer to the segments of the ascending limb of the photopic b-wave (1-1000 Hz bandwidth) which correspond to OP_2 and OP_3 (100-1000 Hz bandwidth) respectively. The OP peak times were all measured from flash onset to the individual peaks of the Ops in the 100-1000 Hz recordings. Analysis was determined only for the days in which 10 or more guinea pigs were evaluated. Statistical significance was determined with the use of the Student t-test, where a $p<0.05$ was considered significant.

Figure 6

Light adapted (30 $cd.m^{-2}$) ERGs (A, right tracing; bandwidth: 1-1000 Hz) and OPs (A, left tracing; bandwidth: 100-1000 Hz) were recorded simultaneously and represent averages of 20 flashes presented at interstimulus intervals of 1.028 sec. Dark adapted ERGs (B, right tracing; 1-1000 Hz) and OPs (B, left tracing; 100-1000 Hz) were recorded simultaneously and represent averages of 2 flashes presented at an interstimulus interval of 1 minute. All tracings were evoked from guinea pigs to a flash intensity of 0.9 log $cd.m^{-2}sec$. The vertical arrow indicates flash onset. Calibration: horizontal: 20 msec; vertical 50 μV (A, left tracing), 10 μV (A, right tracing), 100 μV (B, left tracing), 20 μV (B, right tracing).

A

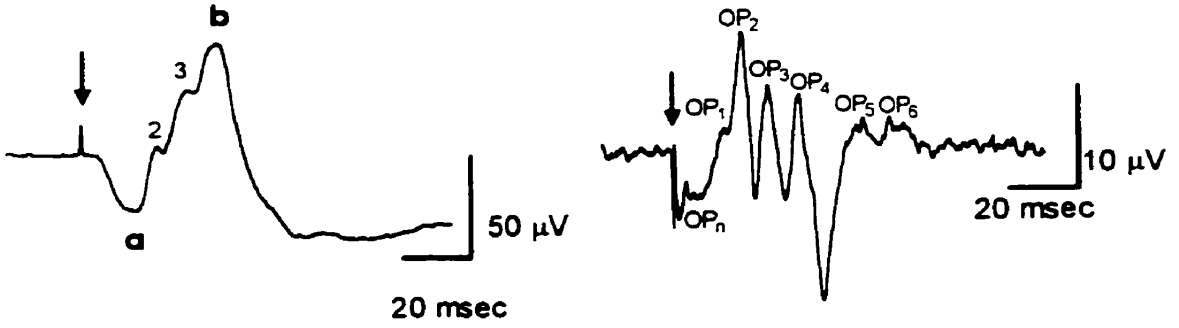
b
3
2
a
50 μV
20 msec
OP2
OP3
OP4
OP1
OP5
OP6
OPn
10 μV
20 msec

B

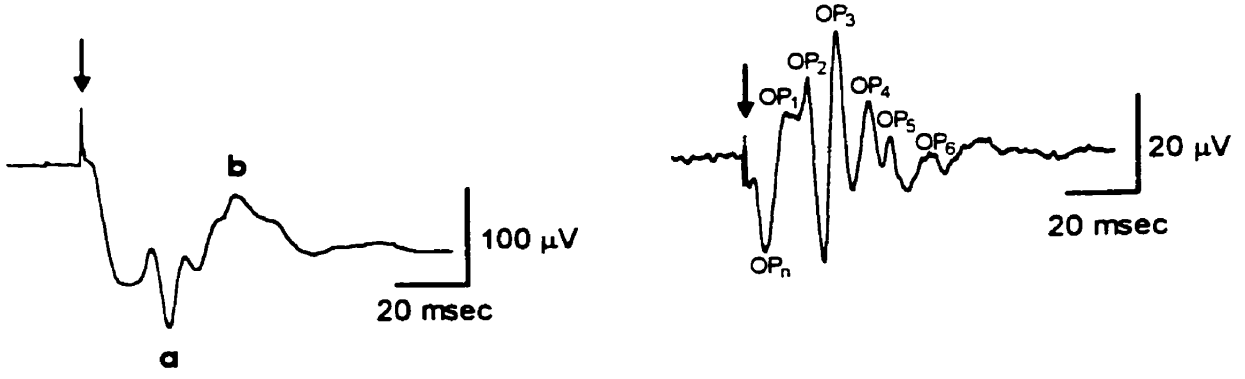
b
a
100 μV
20 msec
OP3
OP2
OP1
OP4
OP5
OP6
OPn
20 μV
20 msec

RESULTS

Maturation of the photopic ERG

Amplitude parameters

To gain a better understanding of the electrophysiological changes that maturation brings to the photopic system of neonatal guinea pig, ERGs and OPs were evoked to a 0.9 log cd.m^{-2}.sec stimulus after they were light adapted to a rod-desensitizing background of 30 cd.m^{-2} for 20 minutes. The stimulus intensity of 0.9 log cd.m^{-2}sec was identified as that which yielded the V_{max} or peak photopic amplitude (photopic hill) as determined with the guinea pig's photopic intensity response function (figure 3).

Representative photopic ERG tracings, obtained during the development of the guinea pig's retina, are exhibited at figure 7. Morphological modifications to the ERG responses (bandwidth: 1-1000 Hz) affected all the ERG components. For example, from ages P_1 to P_{21}, waves 2, and 3 gradually became more prominent components to the ascending limb of the b-wave and consequently its "smooth-like" appearance became "more indented" by P_{21}, suggesting that the OPs became a more prominent feature of the ERG as the retina ages. This is confirmed with the analysis of the OP recordings (bandwidth: 100-1000 Hz) where the amplitudes of the OPs are larger and their overall appearance became a more prominent part of the evoked response with age.

Figure 7

The effect of aging on the photopic (background: 30 $cd.m^{-2}$) ERGs (left tracings of A and B) and OPs (right tracings of A and B) with a bright flash (0.9 $log.cd.m^{-2}$ sec) for two guinea pigs illustrated. P_1 identifies recordings obtained on the day of birth. Recordings obtained on subsequent days are labeled similarly. The ERG (1-1000 Hz bandwidth) and corresponding OPs (100-1000 Hz bandwidth) were recorded simultaneously. The vertical arrow indicates the flash stimulus onset. Calibration: horizontal: 10 msec; vertical 50 μV (left tracings of A and B) 10 μV (right tracings of A and B).

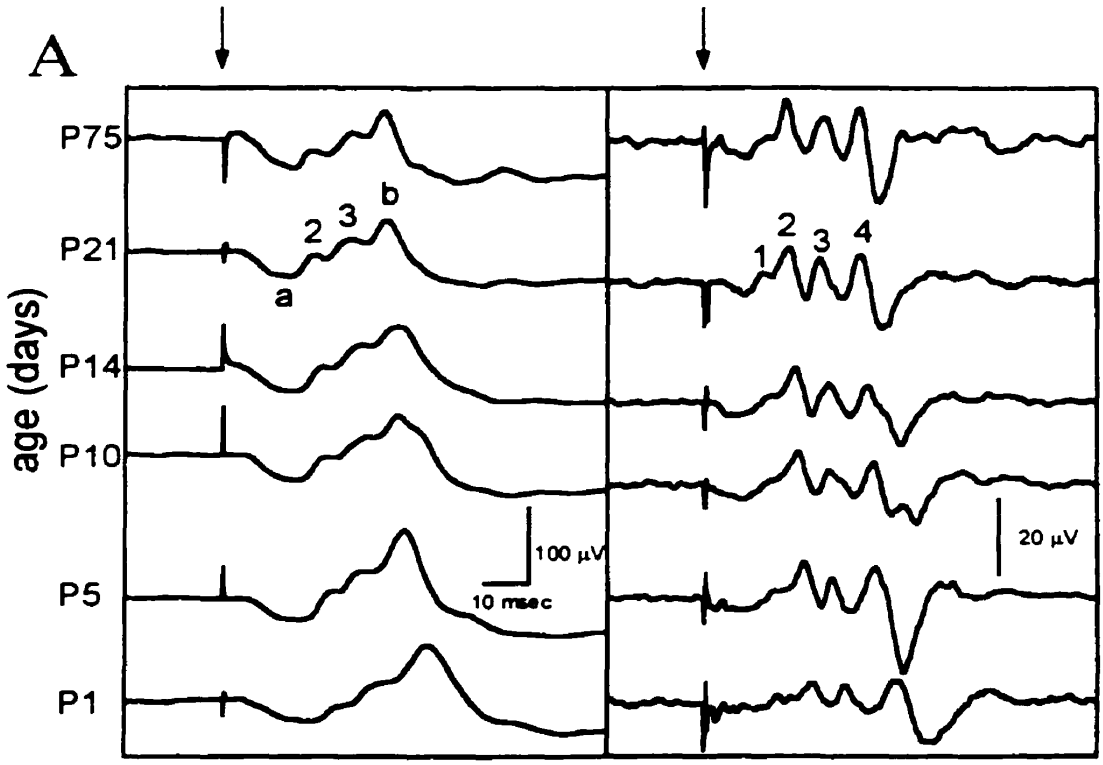
A
P75
P21
P14
P10
P5
P1
age (days)
a
b
2
3
1
2
3
4
100 µV
10 msec
20 µV

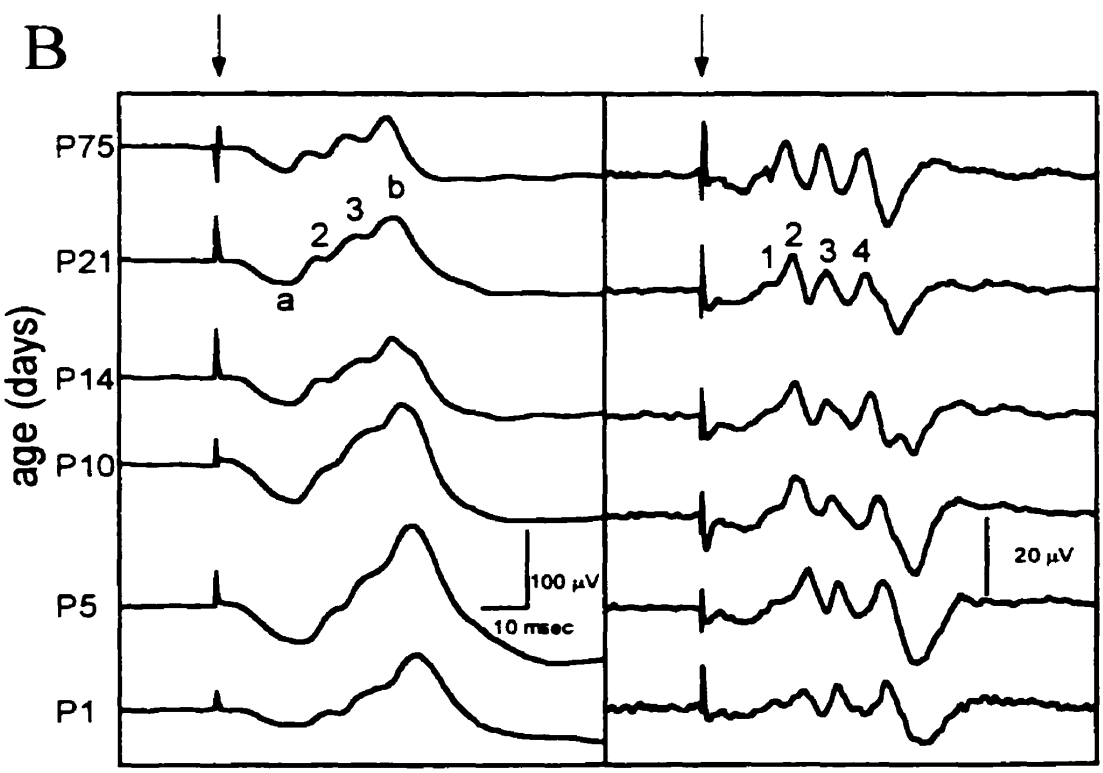
B
P75
P21
P14
P10
P5
P1
age (days)
a
b
2
3
1
2
3
4
100 µV
10 msec
20 µV

Group data of the photopic a- and b-waves and OP responses evoked to a 0.9 log $cd.m^{-2}.sec$ stimulus are plotted against age and summarized at figure 8. As presented in figure 8-A, the amplitude of the b-wave showed a sharp increase from ages P_1 (81.9 $\mu V \pm$ 5.6 μV) to a maximum at age P_5 (132.2 $\mu V \pm 6.0$ μV), after which there was a rapid decline from ages P_5 to P_{14} (74.5 $\mu V \pm 3.8$ μV). After P_{21}, the b-wave amplitude continued to decrease slightly until P_{75} (66.5 $\mu V \pm 1.8$ μV). A significant decrease ($p<0.05$; $n=11$) in the photopic b-wave amplitude was observed between ages P_1 and P_{75}.

The amplitude of the a-wave showed a gradual increase from age P_1 (23.6 $\mu V \pm$ 1.1 μV) to a maximum at age P_{10} (39.6 $\mu V \pm 2.7$ μV), and then decreased to age P_{14} (30.5 $\mu V \pm$ 1.3 μV). However, opposite to that observed for the b-wave, the a-wave amplitude then increased slightly from ages P_{14} (29.7 $\mu V \pm 1.1$ μV) to P_{75} (34.3 $\mu V \pm 1.5$ μV). A significant increase ($p<0.05$; $n=11$) was found between the photopic a-wave amplitude at age P_1 and P_{75}.

Group data obtained from the photopic OPs are presented in figure 8-B and showed a greater complexity compared to the a-wave and b-wave responses described above. Initially OP_2 and OP_4 both displayed a sharp increase in amplitudes from ages P_1 to P_5, while OP_2's amplitude continued to increase to age P_{10}. The amplitudes of OP_3 and OP_4 underwent an abrupt decrease in their amplitudes to age P_{10} and then increased again to P_{21}, the amplitudes of both OP_3 and OP_4 showed increases. However, at P_{21}, the similarities observed between OP_3 and OP_4 ceased: OP_3 decreased slightly from P_{21} (9.8 $\mu V \pm$ 0.3 μV) to P_{75} (9.4 $\mu V \pm 0.3$ μV), whereas OP_4 continued to show a gradual increase to age P_{75} (12.03 $\mu V \pm$ 0.5 μV). As mentioned above, the amplitude of OP_2

Figure 8

Summary of light adapted ERG (A) and OP (B) amplitude measurements with age elicited from a bright flash stimulus (0.9 log $cd.m^{-2}$ sec. Each data point represents the mean ± SEM of measurements obtained from 11 guinea pigs.

A

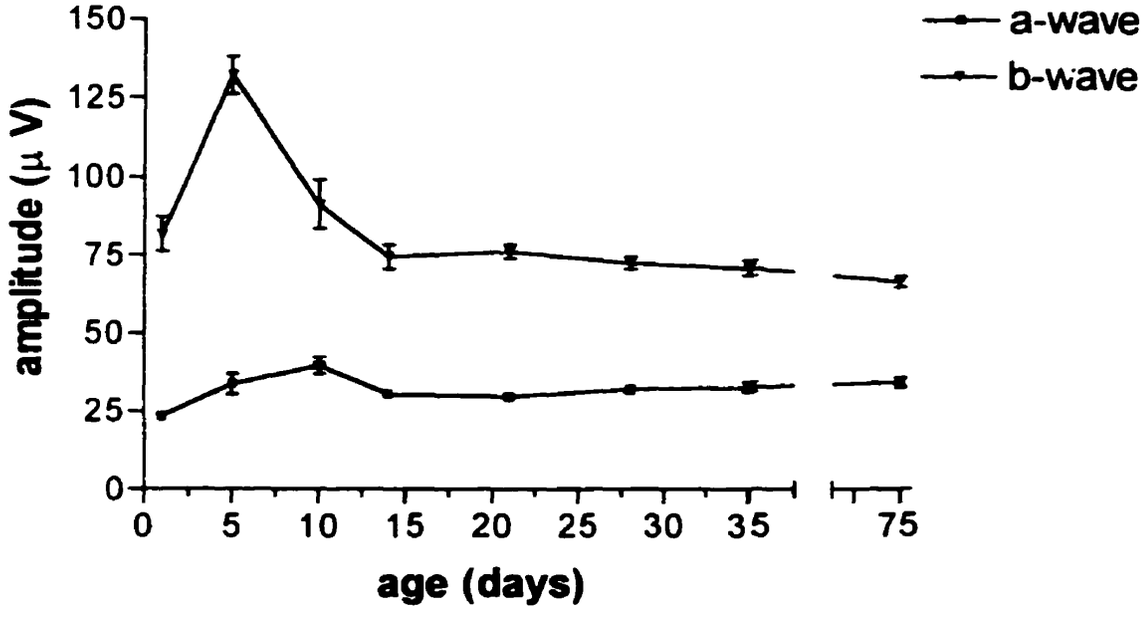
150
125
100
75
50
25
0
amplitude (μ V)
0
5
10
15
20
25
30
35
75
age (days)
a-wave
b-wave

B

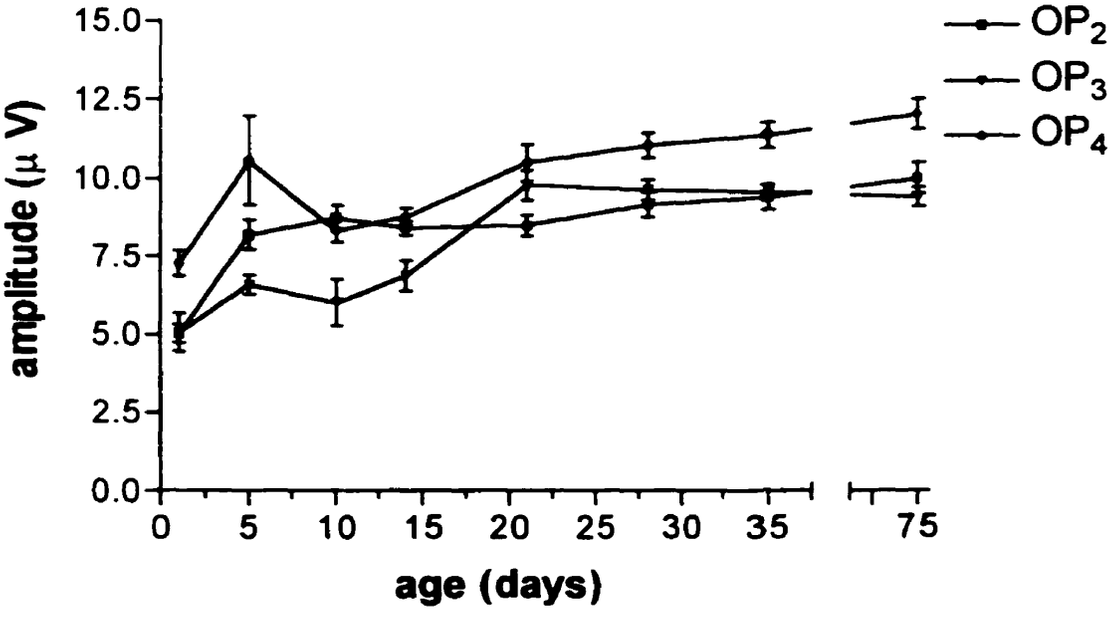
15.0
12.5
10.0
7.5
5.0
2.5
0.0
amplitude (μ V)
0
5
10
15
20
25
30
35
75
age (days)
OP2
OP3
OP4

increased slightly from ages P_5 (8.2 μV ± 0.5 μV) to P_{10} (8.7 μV ± 0.4 μV) and then showed a minor decrease to age P_{21} (8.5μV ± 0.3μV). The amplitude of OP_2 gradually increased from ages P_{21} (8.5 μV ± 0.3 μV) to P_{75} (10.0 μV ± 0.5 μV). Not withstanding the above, it is worthy to note that all OPs showed a significant ($p<0.05$; $n=11$) increase to their amplitudes from ages P_1 to P_{75}.

Peak-time parameters

As summarized in figure 9, the peak times of all photopic ERG components became faster with age. This was most pronounced from ages P_1 to P_{14}. From ages P_{14} to P_{21}, a subtle decrease in the implicit timing was also observed for the b-wave, the a-wave, and OP_2. After P_{21}, there were no further changes to the photopic implicit times which were significantly faster ($p<0.05$; $n=11$) than those measured at P_1. Furthermore there was a significant decrease in the inter-peak interval between the a- and b-waves from ages P_1 to P_{75}, whereas no notable decrease was observed between the inter-peak intervals of the OPs.

b-wave/a-wave parameters

As presented in the introduction, the morphology of the ERG waveform is typically made of a b-wave which has a larger amplitude than the a-wave and consequently the b/a-wave ratio measured in scotopic or photopic conditions is usually above one. As shown in figure 10, the photopic b/a-wave ratio decreased substantially from P_1 (3.51 ± 0.26) to P_{10} (2.11 ± 0.18) but remained positive. After P_{10}, the b/a-wave ratio showed

Figure 9

Summary of light adapted ERG (A) and OP (B) peak-time measurements elicited from a bright flash stimulus (0.9 log $cd.m^{-2}sec$) with age. Each data point represents the mean ± SEM of measurements obtained from 11 guinea pigs.

A

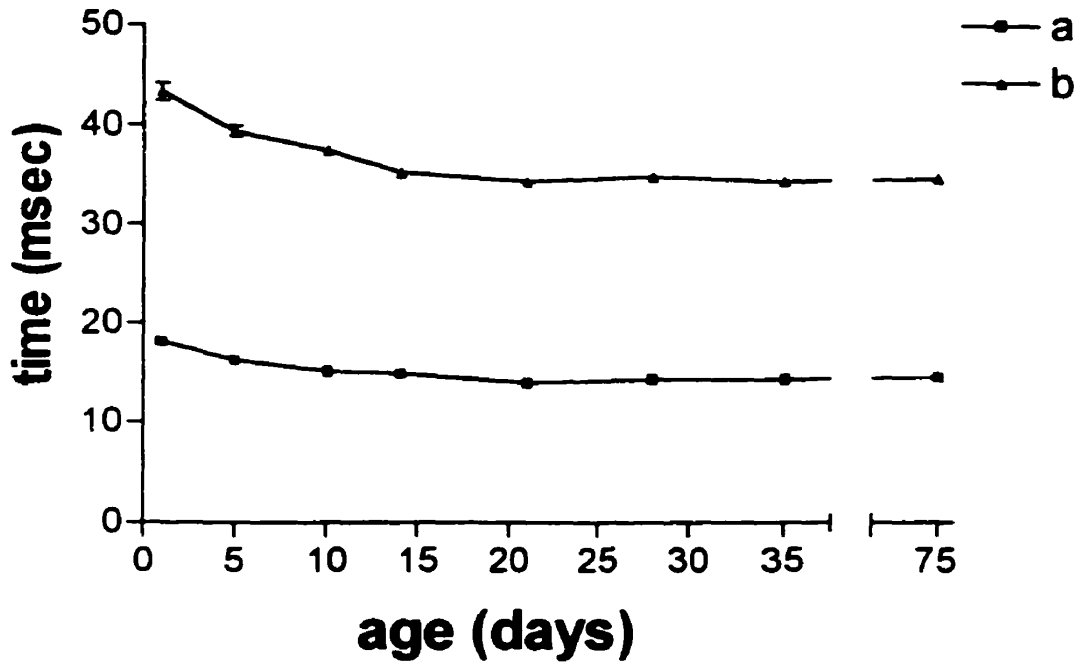
50
40
30
20
10
0
time (msec)
0
5
10
15
20
25
30
35
75
age (days)
a
b

B

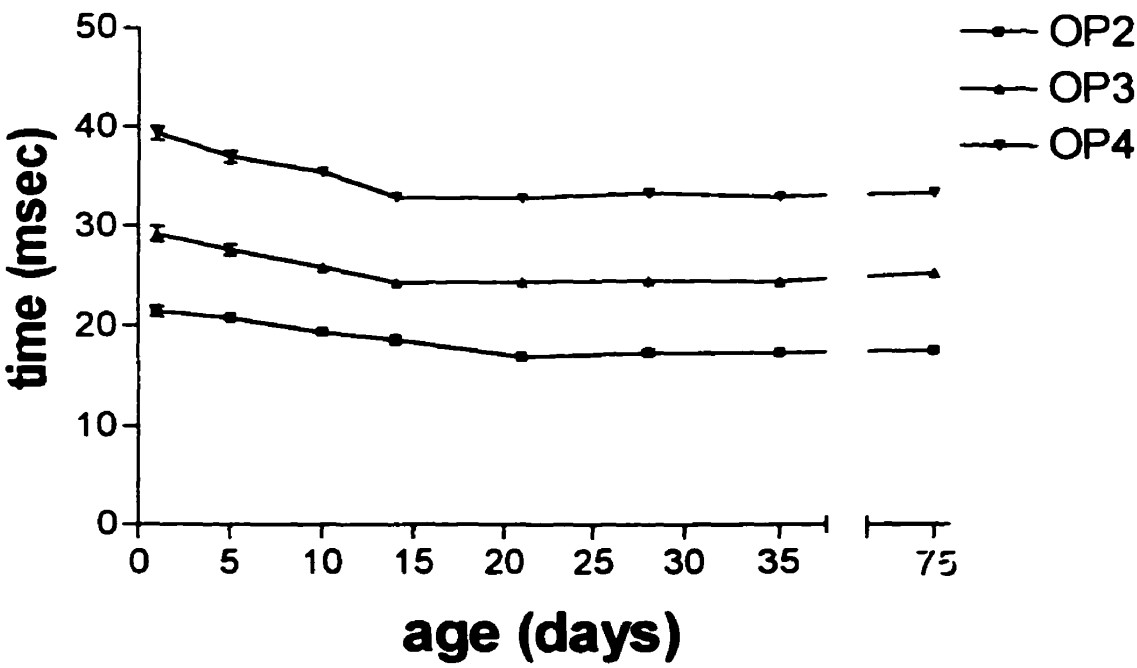
50
40
30
20
10
0
time (msec)
0
5
10
15
20
25
30
35
75
age (days)
OP2
OP3
OP4

Figure 10

The effect of aging on the b-wave/a-wave ratio in light adapted conditions a bright flash stimulus (0.9 log $cd.m^{-2}$ sec). Each bar represents the mean ± SEM of measurements obtained from 11 guinea pigs.

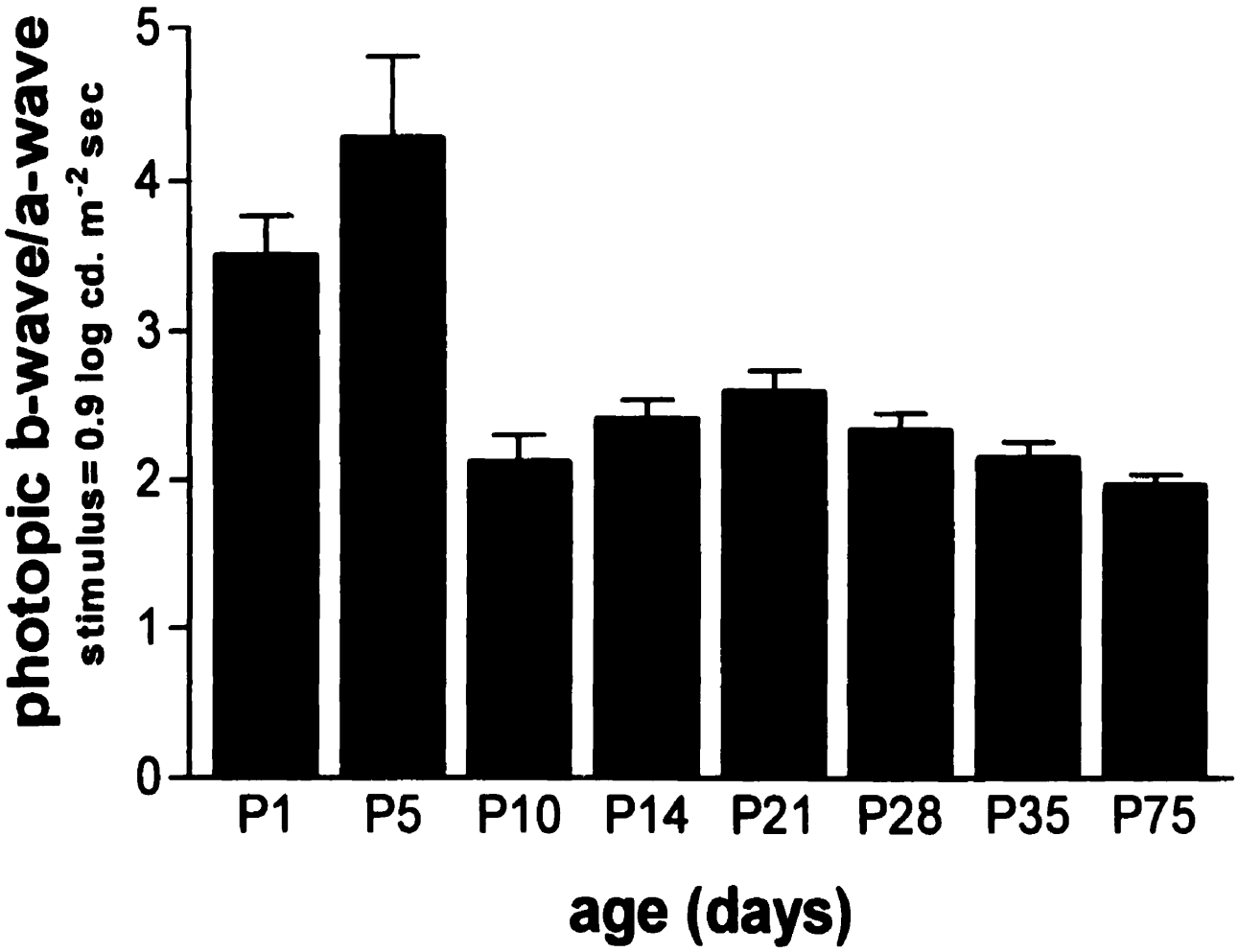
photopic b-wave/a-wave
stimulus= 0.9 log cd. m-2 sec
5
4
3
2
1
0
P1
P5
P10
P14
P21
P28
P35
P75
age (days)

minor fluctuations to its ratio. At P_{75} the photopic b/a-wave ratio was 1.96 ± 0.07, a value significantly lower ($P<0.05$; n=11) than that observed at P_1, but maintaining a ratio above one. The decrease in the ratio from P1 to P75 was the result of an overall decrease in the amplitude of the b-wave combined with an overall increase in the a-wave amplitude.

Light adaptation effect

Following a 12 hour period of dark-adaptation for the guinea pig, an adapting field of 30 $cd.m^{-2}$ was opened and photopic ERGs and OPs were obtained. Representative tracings of the light adaptation effect (LAE) evoke at age P_1 are presented at figure 11-A.

The LAE response obtained from the same guinea pig at age P_{75} are shown at figure 11-B. Neither the neonatal guinea pig nor the adult guinea pig exhibited an enhancement of the ERG or a progressive decrease in peak times with increasing light adaptation. Group data recorded at P_1 and P_{75} are presented in figure 11-C, where the mean amplitude of the b-wave (expressed as a percentage change in ERG amplitude) is plotted against the length of the light adaptation period. At age P_1, the b-wave at t_0 was 102.6% ± 1.8% compared with 96.8% ± 1.7% at t_{15}. These values were not statistically different ($p<0.05$; n=11) from one another. Results obtained at age P_{75} were essentially the same: at t_0, the b-wave was 103.6% ± 1.9% compared with 97.5% ± 3.0% at t_{15}. Again the values are not statistically different ($p<0.05$; n=11) from one another. Futhermore, similar results obtained at ages P_1 and P_{75} (figure 11-D) did not display the LAE. Irrespective of age, the guinea pig did not display b-wave or OP_4 enhancements previously shown to occur with other species investigated as mentioned in the introduction.

Figure 11

Photopic (background: 30 $cd.m^{-2}$) ERGs (left tracings of A and B;1-1000 Hz bandwidth) and OPs (right tracings of A and B;100-1000 Hz bandwidth) recorded simultaneously and evoked to a bright flash (0.9 log $cd.m^{-2}sec$) delivered immediately following a 12 hour period of dark adaptation. Responses in A and B show the first 20 minutes of light adaptation obtained from a guinea pig at P_1 (day of birth) and P_{75}, respectively, where t= time of light adaptation in minutes. The vertical arrow indicates the flash stimulus onset. The b-wave amplitudes recorded at age P_1 and at age P_{75} are summarized in C (ordinate: percentage of b-wave amplitude after 20 minutes of light adaptation to the adapting field) and OP_4 amplitudes recorded at age P_1 and at age P_{75} are summarized in D (ordinate: percentage of OP4 after 20 minutes of light adaptation to the adapting field). The results of each guinea pig was normalized individually. Each data point represents the mean ± SEM of measurements obtained from 11 guinea pigs. Calibration: horizontal: 10 msec (A and B); vertical 50 μV (left tracings of A and B) 10 μV (right tracings of A and B).

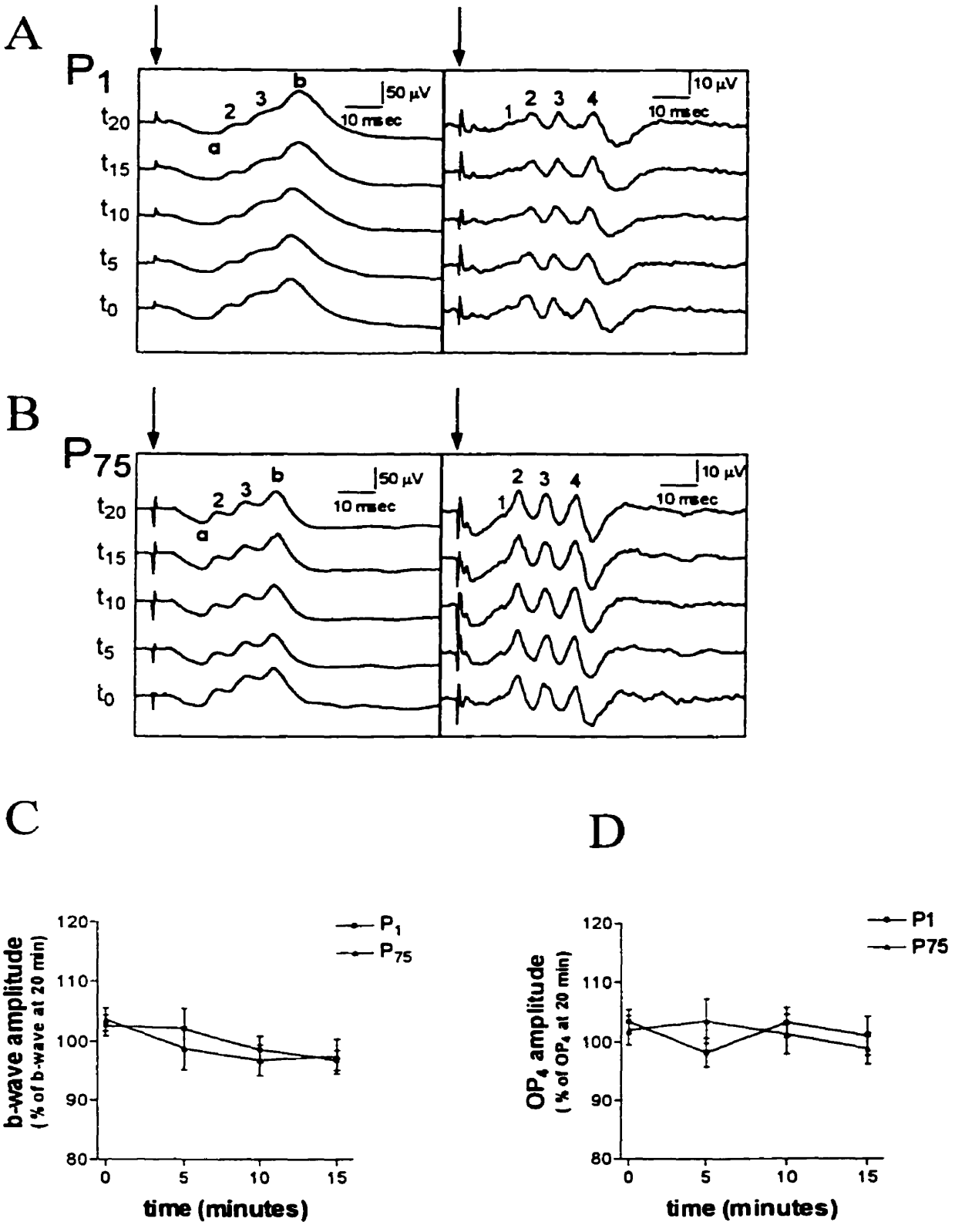
A
P1
t20
t15
t10
t5
t0
a
b
2
3
50 µV
10 msec
1
4
10 µV
B
P75
C
D
b-wave amplitude
(% of b-wave at 20 min)
120
110
100
90
80
0
5
10
15
time (minutes)
P1
P75
OP4 amplitude
(% of OP4 at 20 min)

slow flicker parameters

The maturation of the photopic OP reposnes was also investigated with the use of a flickering stimulus. Illustrated in figure 12-A and 12-B are the photopic OP tracings evoked from three neonatal guinea pigs (24 to 48 hours after birth) and three older guinea pigs at P_{75}. Amplitudes and peak time measurements are summarized at figure 13.

Differences between ERG responses were noticed for all OPs evoked between the two age groups of guinea pigs, but these differences were often dependent on the rate of presentation. For example, the amplitude of OP_3 evoked to a 0.5 Hz flicker was significantly smaller ($p<0.05$; $n=11$) for neonatal guinea pigs than for guinea pigs at age P_{75}. As the rate of presentation increased to 8 Hz, abrupt decreases to the amplitude of OP_3 was observed for both groups. However, as can be seen in figure 12, neonatal guinea pigs almost never produced an OP_3 response for frequencies of 8 Hz and above, whereas guinea pigs at age P_{75} often displayed a small but noticeable OP_3 response. Of the 11 guinea pigs analyzed at P_{75}, 7 guinea pigs had a noticeable OP_3 at 8 Hz. As the rate of presentation was increased from 8 Hz to 16 Hz, a complete abolishment was observed in all but four guinea pigs aged P_{75}.

The neonatal guinea pig and the guinea pig at P_{75} both exhibited an overall peak time shortening of OP_3 as the flicker rate was increased from 0.5 Hz to 8 Hz. There was no difference in the timing for these two groups of guinea pigs at a rate of presentation of 0.5 Hz ($p=0.85$; $n=11$).

The response of OP_2 to a flickering stimulus was noticeably different than OP_3, as OP_2 was more resistant to a flickering stimulus at a higher rate of presentation. For the neonatal guinea pig, the amplitude of OP_2 increased as the rate of presentation was

Figure 12

Light adapted (30 cd.m-^{2}) OPs obtained from 3 neonatal guinea pigs (A) and 3 guinea pig at age P_{75} (B) evoked to a bright flash stimuli (0.9 log cd.m^{-2} sec). Tracings represent averages of 50 flashes presented at an interstimulus interval of 0.5, 1, 2, 4, 8, and 16 Hz. The vertical arrow indicates the flash stimulus onset. Calibration: horizontal: 20 msec; vertical 15 μV.

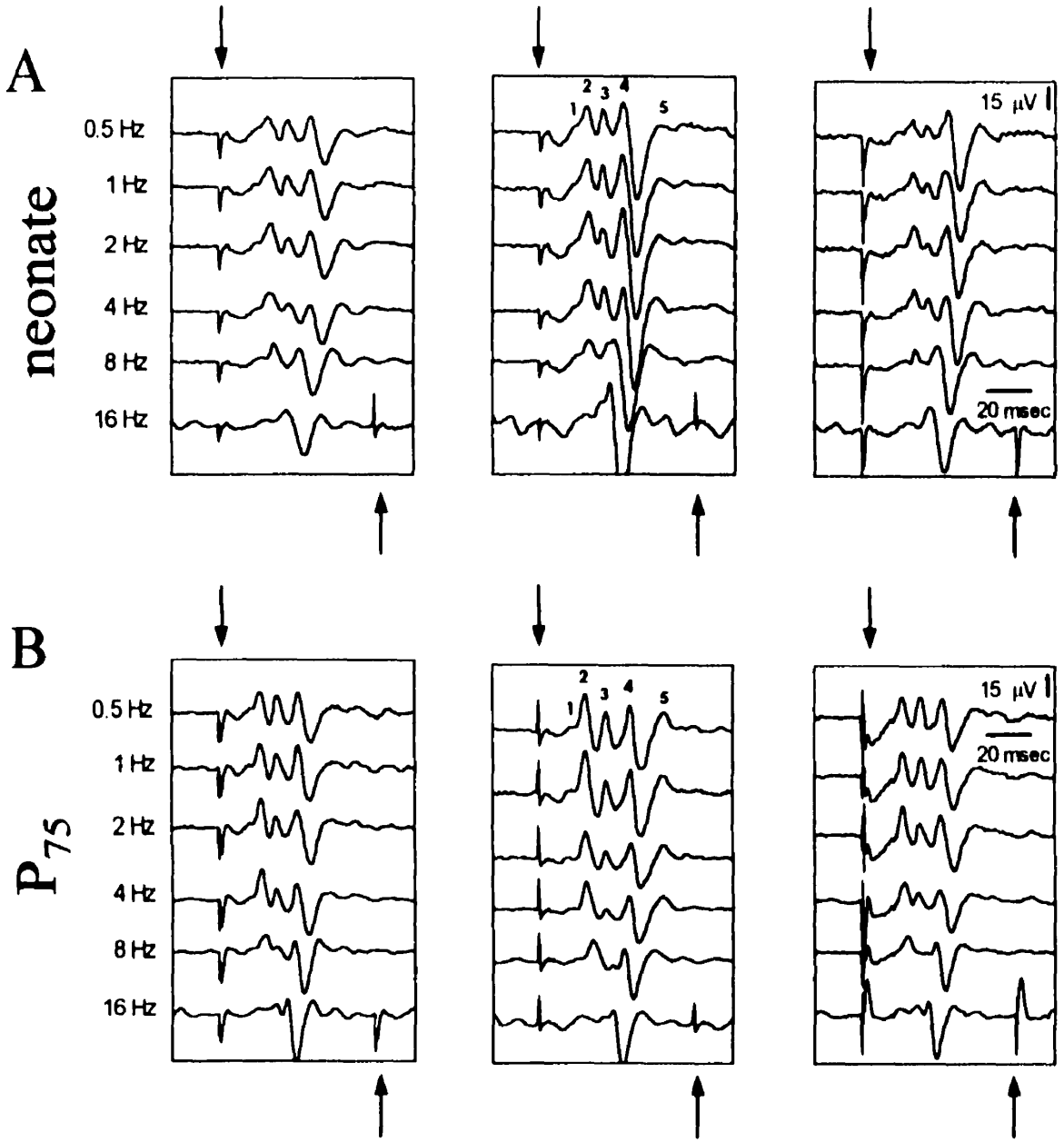
A
neonate
0.5 Hz
1 Hz
2 Hz
4 Hz
8 Hz
16 Hz
1
2
3
4
5
15 μV
20 msec
B
P75
0.5 Hz
1 Hz
2 Hz
4 Hz
8 Hz
16 Hz
1
2
3
4
5
15 μV
20 msec

Figure 13

The effect of a flickering stimulus on photopic (background: 30cd.m^{-2}) OPs evoked to bright flash stimuli (0.9 log cd.m^{-2} sec.) delivered at 0.5, 1, 2, 4, 8, and 16 Hz. The recordings were obtained from neonatal (represented by a square symbol; n=11) and adult (represented by a triangle symbol; n=11) guinea pigs. The left graphs of A, B, and C summarize the amplitudes of OP_2, OP_3, and OP_4 respectively. The right graphs of A, B, and C summarize the implicit-times of OP_2, OP_3, and OP_4 respectively. The abscissa represents the presentation rate of the stimulus given in Hz.

A

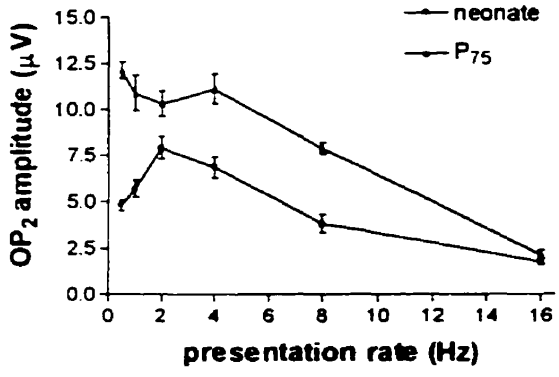
neonate
P75
OP2 amplitude (μV)
15.0
12.5
10.0
7.5
5.0
2.5
0.0
0 2 4 6 8 10 12 14 16
presentation rate (Hz)

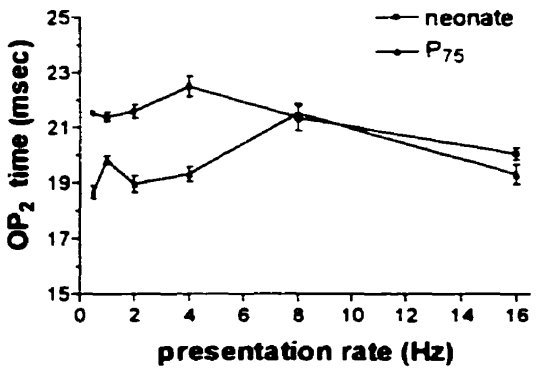
neonate
P75
OP2 time (msec)
25
23
21
19
17
15
0 2 4 6 8 10 12 14 16
presentation rate (Hz)

B

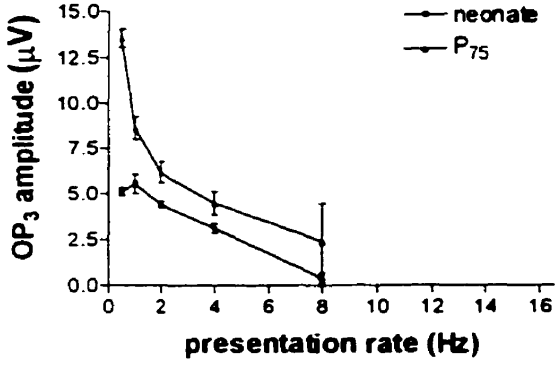
neonate
P75
OP3 amplitude (μV)
15.0
12.5
10.0
7.5
5.0
2.5
0.0
0 2 4 6 8 10 12 14 16
presentation rate (Hz)

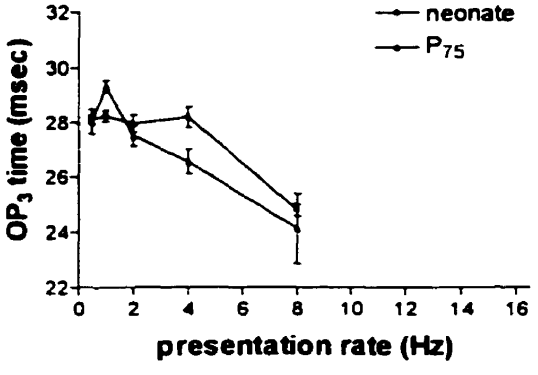
neonate
P75
OP3 time (msec)
32
30
28
26
24
22
0 2 4 6 8 10 12 14 16
presentation rate (Hz)

C

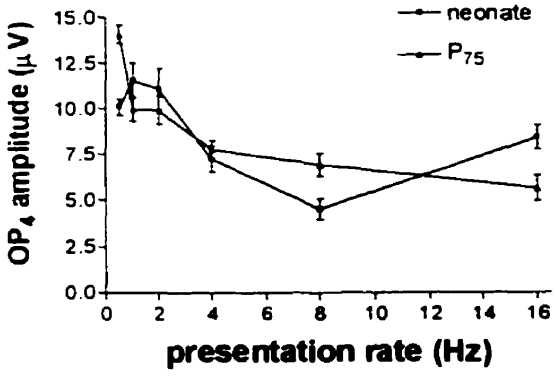
neonate
P75
OP4 amplitude (μV)
15.0
12.5
10.0
7.5
5.0
2.5
0.0
0 2 4 6 8 10 12 14 16
presentation rate (Hz)

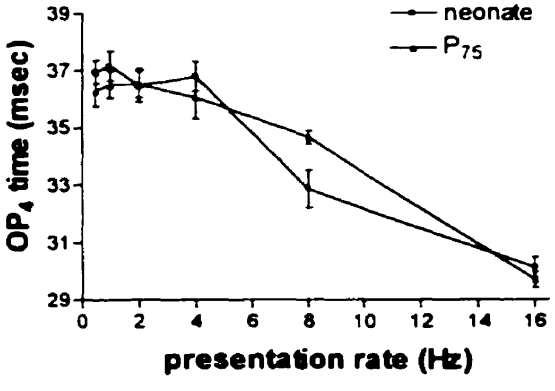
neonate
P75
OP4 time (msec)
39
37
35
33
31
29
0 2 4 6 8 10 12 14 16
presentation rate (Hz)

increased from 0.5 Hz to 2 Hz (figure 13-A). In response to a further increase to 16 Hz, 1 of the 11 guinea pigs showed no OP_2 response, while reduced amplitudes were observed in the other neonatal guinea pigs. The amplitude behavior of OP_2 recorded at age P_{75} was different from that of the neonate as it showed a decline (with a minor amplitude increase from 2 Hz to 4 Hz) as the rate of flicker presentation increased from 0.5 to 16 Hz. A notable, but small OP_2 response was observed in all guinea pigs at age P_{75} when evoked to a flicker presentation of 16 Hz. A marked increase ($p<0.05$; $n=11$) in amplitude and a decrease ($p<0.05$; $n=11$) in timing of OP_2 was observe for guinea pigs with age.

The response of OP_4 evoked to a 16 Hz flicker presentation was found to be the most resistant of all the OPs. Both age groups displayed an overall decrease in amplitude as the rate of presentation was increased from 0.5 Hz to 8Hz. The amplitude of OP_4 at age P_{75} continued to decrease to a flicker rate of 16 Hz, whereas the amplitude of OP_4 in the neonate abruptly increased to the same presentation. The amplitude of OP_4 evoked to a 16 Hz flicker was markedly larger ($p<0.05$; $n=11$) for the neonate then at age P_{75}.

The timing of OP_4 for both the neonatal guinea pig and the guinea pigs at P_{75} was similar. In general, as the rate of presentation was increased from 0.5 Hz to 16 Hz, the peak time for both age groups decreased. No difference ($p<0.05$; $n=11$) was found in the timing for OP_4 between these two groups of guinea pigs for a presentation rate of 0.5 Hz ($p= 0.36$, $n= 11$) or 16 Hz ($p= 0.35$, $n= 11$).

Maturation of the scotopic ERG

Amplitude parameters

Scotopic intensity response functions obtained from 2 different guinea pigs at P_1, P_5, P_{10}, and P_{75} are shown at figure 14. The b-wave was first observed at a flash intensity about –3.9 log.cd.m^{-2} sec. Further increases in intensity, in 0.3 log unit steps, resulted in a gradual increase in the b-wave amplitude and a concurrent shortening in the b-wave implicit time. ERGs evoked with brighter flashes continued to exhibit this behavior until the stimulus was approximately –2.4 log cd.m^{-2} sec.

Between -2.4 and -1.2 log cd.m^{-2} sec, the b-wave amplitude failed to grow as the flash stimulus was increased. In fact, brighter stimuli resulted in smaller b-wave amplitudes until the flash stimulus reached -1.2 log cd.m^{-2} sec. As the stimulus is increased from -1.2 log cd.m^{-2} sec to 0.9 log cd.m^{-2} sec the amplitude of the b-wave exhibited yet another behavior. Once again, increments to the flash intensity greater than -1.2 log cd.m^{-2} resulted in a gradual increase in the b-wave amplitude. Furthermore, and similar to what was noted for the photopic responses, the amplitude of the b-wave goes through a maximum amplitude before showing a decrease with age, irrespective of the intensity used (figure 15).

To summarize, with an increasing flash stimulus, the b-wave amplitude increased at dim stimuli, decreased at mid-range flash intensities, and finally increased again with the brightest flashes used in this study. The overall result was an intensity-response curve with a bimodal growth as shown at figure 16A.

Figure 14

The effect of aging on the scotopic intensity response function for the ERG (1-1000 Hz bandwidth) and OPs (100-1000 Hz bandwidth) for two guinea pigs illustrated. In A and B, ERGs (left tracings) and OPs (right tracings) were evoked to flashes of white light of increasing flash intensities spanning over a 6 log unit range with the maximum flash being 0.9 log.cd.m^{-2}.sec in energy. P_1 identifies recordings obtained on the first day of birth. Recordings obtained on subsequent days are labeled similarly. The vertical arrow indicates the flash stimulus onset. Calibration: horizontal: 20 msec; vertical: 75 μV (left tracings of A and B), 15 μV (right tracings of A and B).

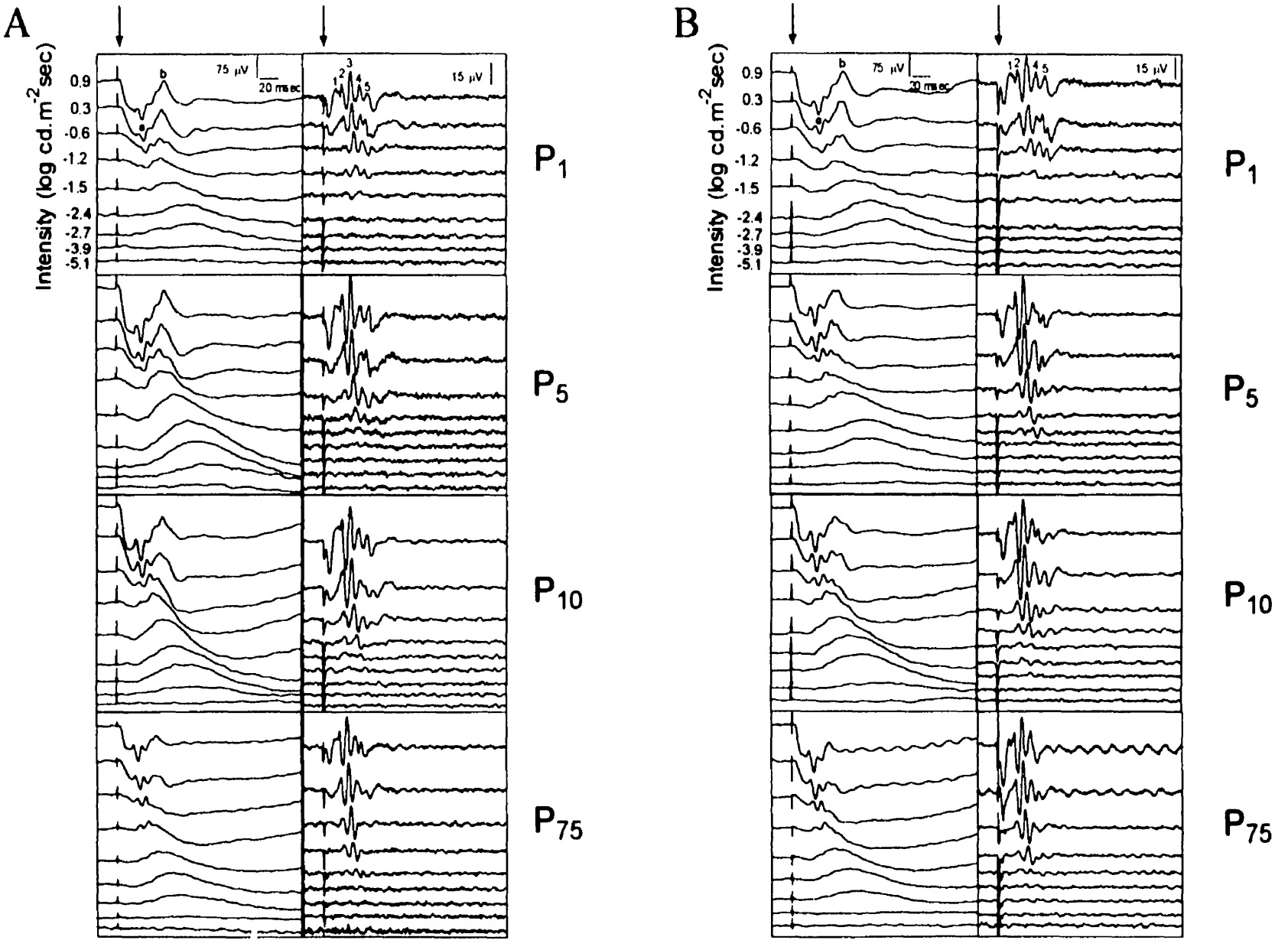
A
B
Intensity (log cd.m-2sec)
0.9
0.3
-0.6
-1.2
-1.5
-2.4
-2.7
-3.9
-5.1
b
75 µV
20 msec
1
2
3
4
5
15 µV
P1
P5
P10
P75

Figure 15

The effect of aging on the scotopic ERG (1-1000 Hz bandwidth) and OPs (100-1000 Hz bandwidth) for two guinea pigs illustrated. In A and B, ERGs (left tracings) and OPs (right tracings) were evoked to flashes of white light 0.6 log.cd.m^{-2}.sec (upper tracings), -0.9 log.cd.m^{-2}.sec (middle tracings), and –2.4 log.cd.m^{-2}.sec (lower tracings). P_1 identifies recordings obtained on the first day of birth. Recordings obtained on subsequent days are labeled similarly. The vertical arrow indicates the flash stimulus onset. Calibration: horizontal: 20 msec; vertical: 75 μV (left tracings of A and B), 15 μV (right tracings of A and B).

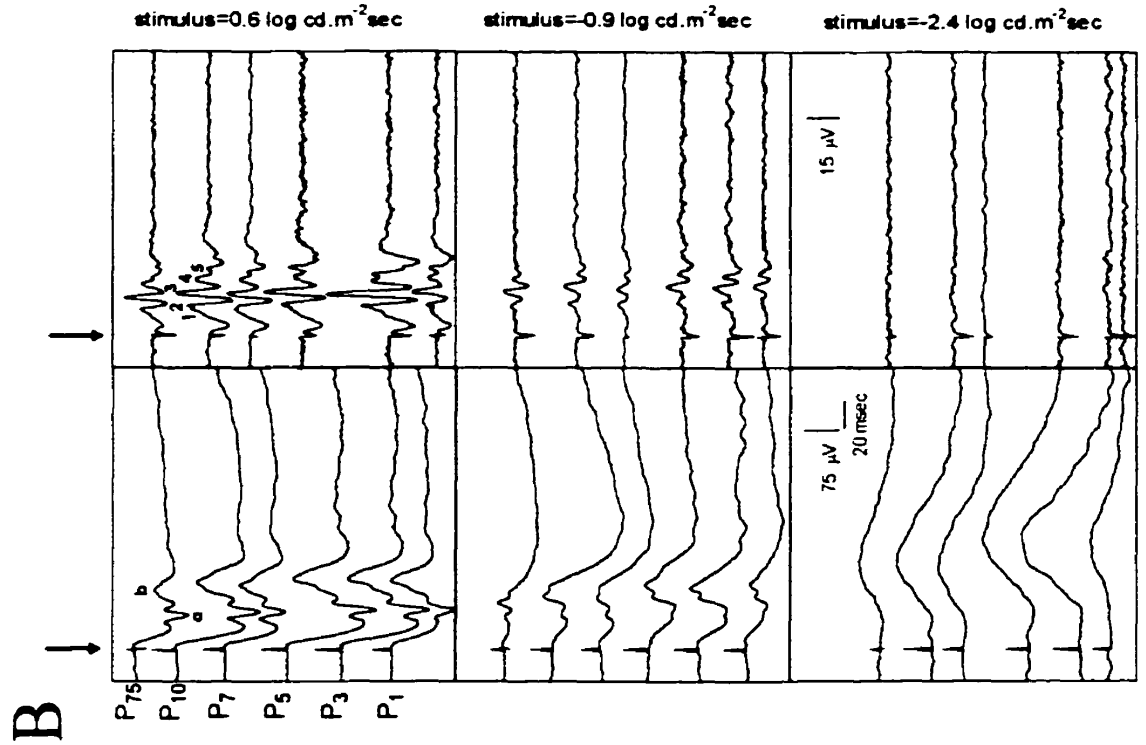
stimulus=0.6 log cd.m-2sec
stimulus=-0.9 log cd.m-2sec
stimulus=-2.4 log cd.m-2sec
15 µV
75 µV
20 msec
P75
P10
P7
P5
P3
P1
B

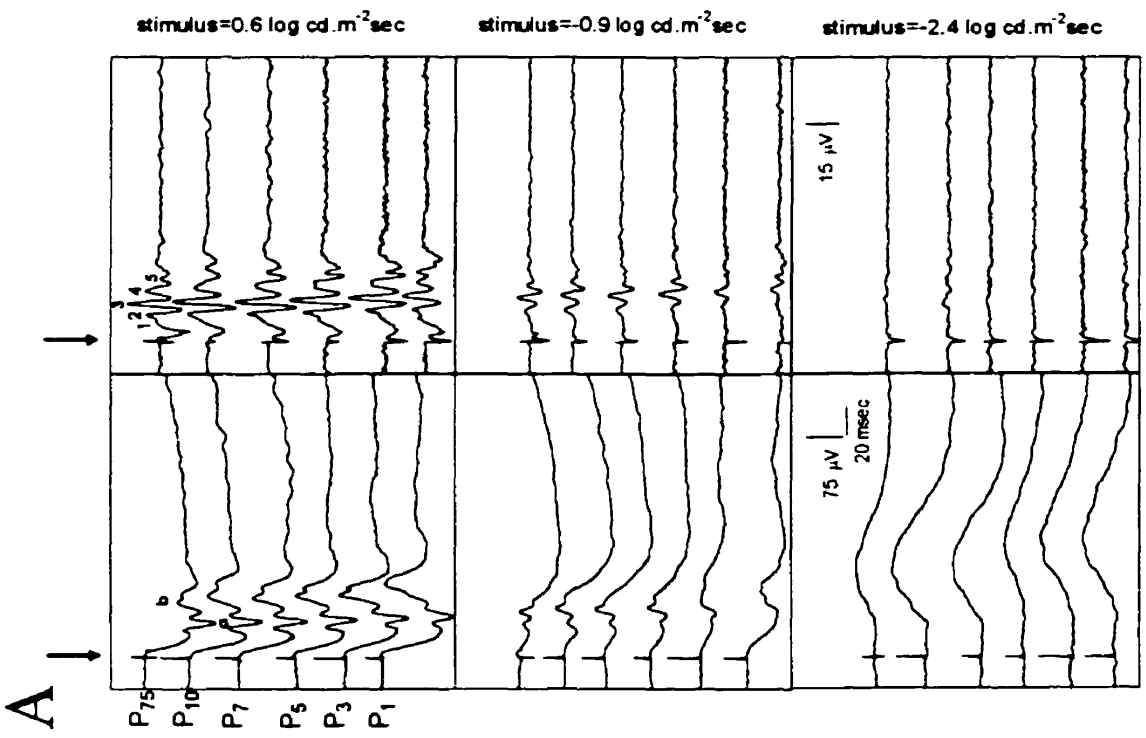
stimulus=0.6 log cd.m-2sec
stimulus=-0.9 log cd.m-2sec
stimulus=-2.4 log cd.m-2sec
15 µV
75 µV
20 msec
P75
P10
P7
P5
P3
P1
A

Figure 16

Summary of intensity-response curves of the dark-adapted guinea pig for different ages. Scotopic b-wave amplitude measurements at the corresponding flash intensity are presented in A. Scotopic a-wave amplitude measurements at the corresponding flash intensity are presented in B. Symbols in A and B identifying the day on which the results were obtained. An adult scotopic intensity-response curve is shown in C. Each data point represents the mean ± SEM of measurements obtained from 11 guinea pigs.

A

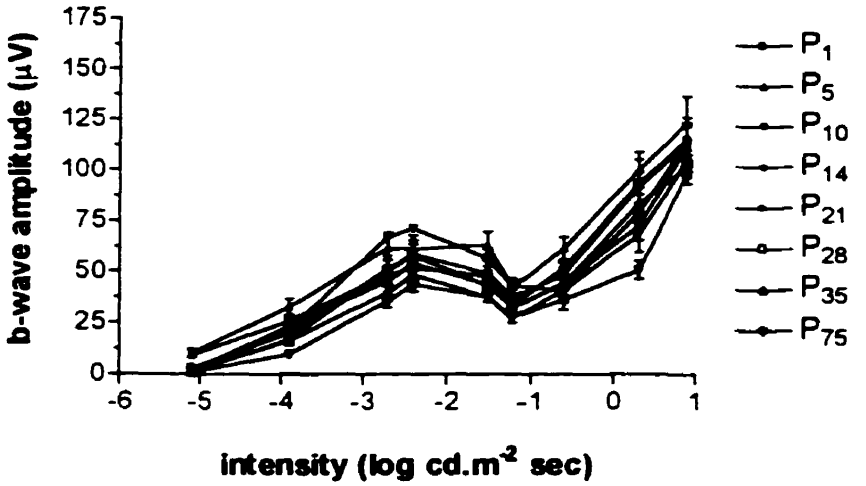
b-wave amplitude (μV)
175
150
125
100
75
50
25
0
-6
-5
-4
-3
-2
-1
0
1
intensity (log cd.m-2 sec)
P1
P5
P10
P14
P21
P28
P35
P75

B

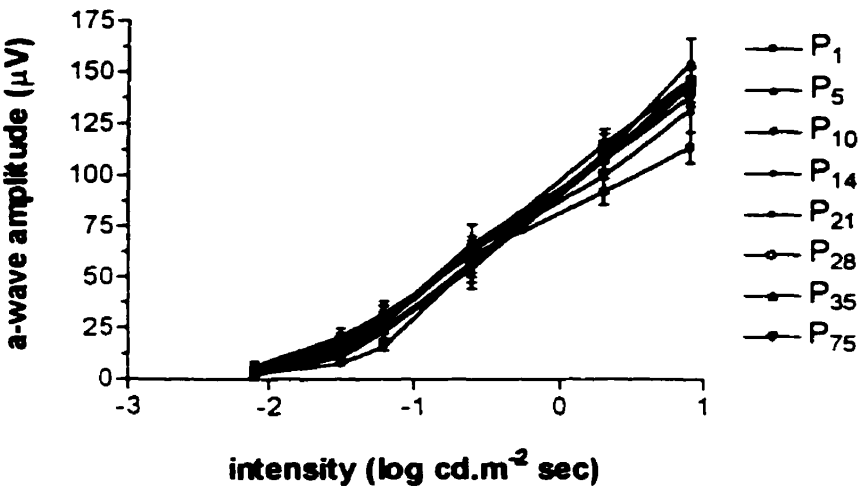
a-wave amplitude (μV)
175
150
125
100
75
50
25
0
-3
-2
-1
0
1
intensity (log cd.m-2 sec)
P1
P5
P10
P14
P21
P28
P35
P75

C

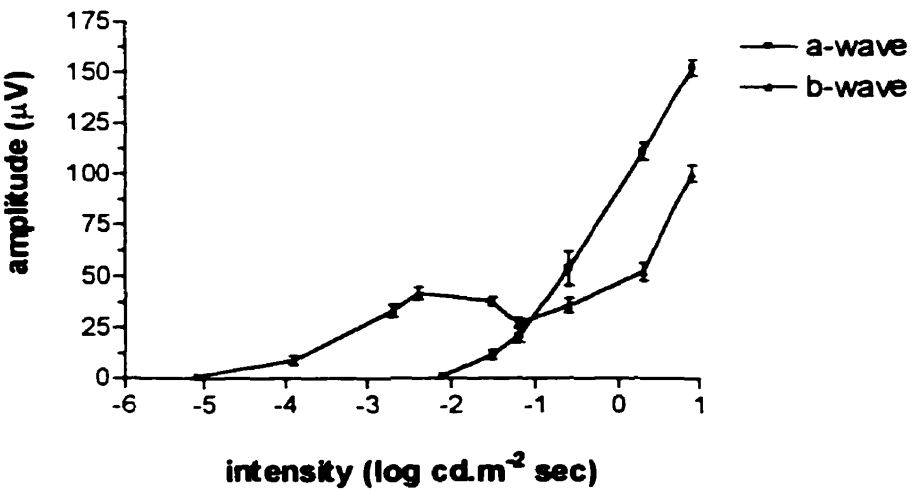
amplitude (μV)
175
150
125
100
75
50
25
0
-6
-5
-4
-3
-2
-1
0
1
intensity (log cd.m-2 sec)
a-wave
b-wave

At figure 14, representative intensity response function tracings show that a flash stimulus of approximately –2.1 log cd.m^{-2} sec or higher is needed to evoke a scotopic a-wave response in the guinea pig. An increase to the flash stimulus beyond the a-wave threshold evoked an a-wave of larger amplitude, regardless of age (figure 14). Group data in figure 16-B and 16-C shows that the a-wave amplitude increased linearly, where the largest a-wave amplitude observed is produced at the brightest stimulus intensity.

The results shown at figure 14 include OP responses. Regardless of age, OP_3 was usually the first OP to be evidenced at a flash stimulus between –2.4 and –1.5 log cd.m^{-2} sec. Like the a-wave mentioned above, an increment to the flash stimulus evoked an OP_3 response with larger amplitudes, regardless of age (figure 14). Moreover, of all the OPs, OP_3 was observed to have the greatest amplitude at any stimulus intensity.

To illustrate further the effect of maturation on the scotopic function, a-wave, b-wave, and OP amplitudes, evoked to a stimulus of 0.9 log cd.m^{-2} sec, were plotted against age. As shown in figure 17-A, all ERG components changed between ages P_1 and P_{21}. There was a sharp increase to the amplitude of the a-wave from ages P_1 (114.0 μV ± 7.5 μV) to a maximum at P_{14} (154.8 μV ± 12.4 μV). From ages P_{14} to P_{21} the amplitude of the a-wave gradually decreased. In comparison, the amplitude of the b-wave increased to a maximum of 123.0 μV ± 13.4 μV at P_5 and then showed an overall decrease to P_{21} (104.5 μV ± 4.1 μV). Both the a-wave and b-wave amplitudes stabilized and remained relatively constant after P_{21}. Overall, the a-wave demonstrated a significant increase ($p<0.05$; $n=11$) between ages P_1 and P_{75}. In contrast, there was a small but not significant ($p=0.101$; $n=11$) reduction in b-wave amplitudes between ages P_1 and P_{75}.

Figure 17

Summary of dark-adapted ERG (A) and OP (B) amplitude measurements with age elicited from a bright flash stimulus (0.9 log $cd.m^{-2}.sec$). Each data point represents the mean ± SEM of measurements obtained from 11 guinea pigs.

A

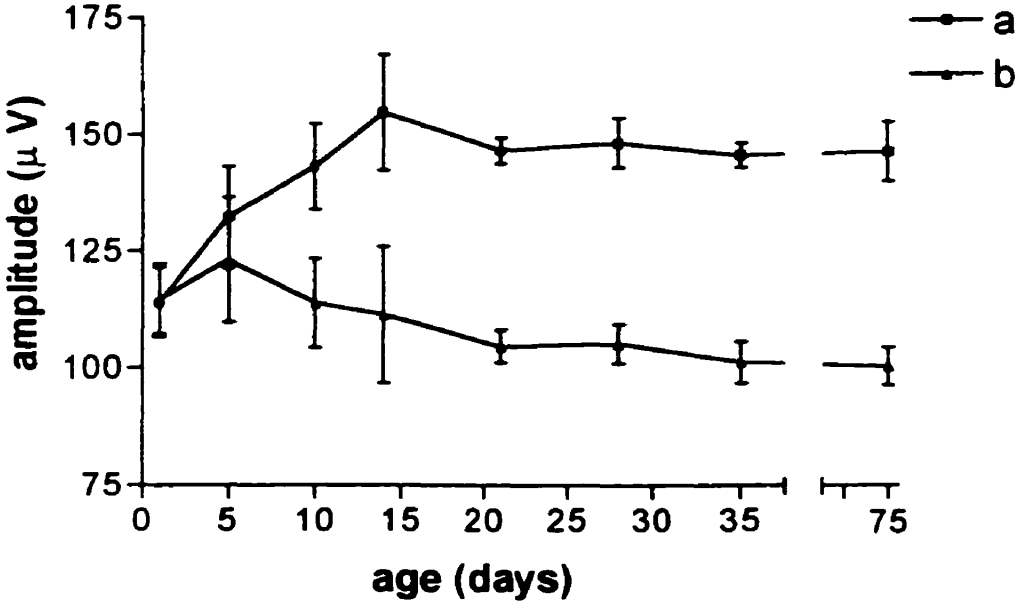
175
150
125
100
75
amplitude (μ V)
0
5
10
15
20
25
30
35
75
age (days)
a
b

B

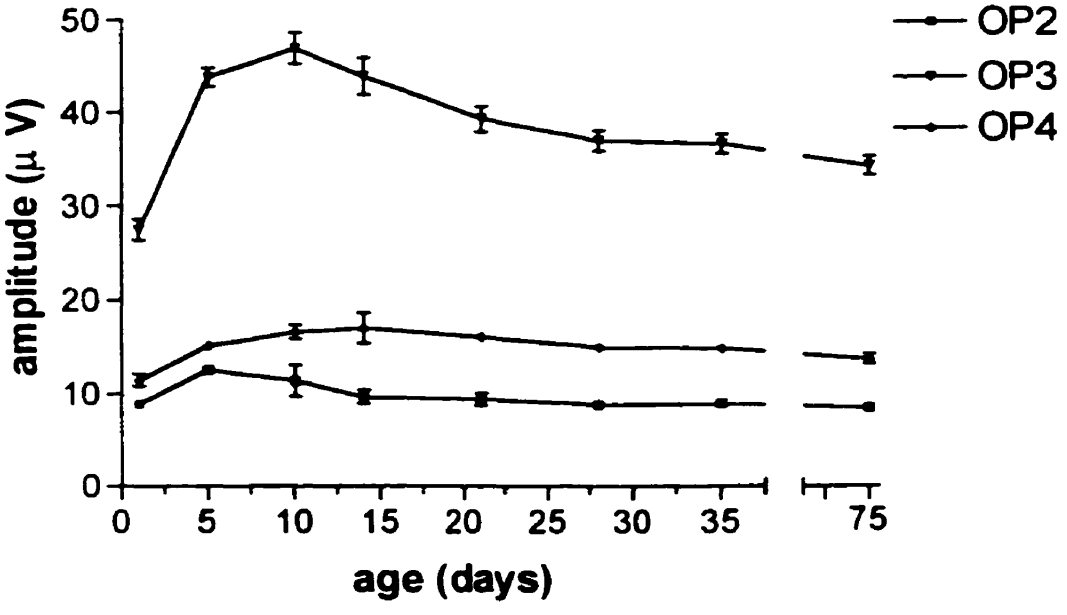
50
40
30
20
10
0
amplitude (μ V)
0
5
10
15
20
25
30
35
75
age (days)
OP2
OP3
OP4

The OPs were also markedly modified between ages P_1 and P_{28} (Figure 17-B). The most pronounced of these changes affected OP_3. The amplitude of OP_3 increased from age P_1 (27.5 μV ± 1.1 μV) to a maximum at age P_{10} (43.9 μV ± 2.0 μV). The amplitude of OP_3 then gradually decreased between ages P_{10} and P_{28}, (37.0 μV ± 1.0 μV) after which it remained relatively stable. Overall, a significant increase ($p<0.05$; $n=11$) in amplitude was observed for OP_3 between the ages P_1 and P_{75}. The amplitude of OP_2 displayed an increase from age P_1 (8.8 μV ± 0.2 μV) to a maximum at age P_5 (12.5 μV ± 0.3 μV). However, the amplitude of OP_2 gradually decreased from ages P_5 to P_{14} (9.7 μV ± 0.7 μV) after which its amplitude stabilized. There was no difference ($p=0.44$; $n=11$) in the amplitude of OP_2 between ages P_1 and P_{75}. The amplitude of OP_4 gradually increased from ages P_1 (11.5 μV ± 0.6 μV) to a maximum at age P_{14} (17.0 μV ± 1.7 μV). The amplitude of OP_4 displayed a slight decrease until it stabilized at P_{28} (15.0 μV ± 0.5 μV). There was a significant increase ($p<0.05$; $n=11$) in the amplitude of OP_4 from ages P_1 to P_{75}.

Peak-time parameters

A summary of the implicit times for the ERG and OP components elicited with the brightest stimulus (0.9 log $cd.m^{-2}.sec$) and delivered in scotopic conditions are shown in figure 18-A and 18-B. A similar behavior in timing was observed between the b-wave and OP_4. The implicit time for both these components lengthened to age P_5 and then shortened to age P_{14}. Furthermore, both the b-wave and OP_4 continued to similarly display slight decreases in their timing until P_{35} where their implicit times stabilized. The peak times of the a-wave, OP_2, and OP_3 collectively exhibited the same behavior. These components

Figure18

Summary of dark-adapted ERG (A) and OP (B) peak-time measurements with age elicited from a bright flash stimulus (0.9 log $cd.m^{-2}.sec$). Each data point represents the mean ± SEM of measurements obtained from 11 guinea pigs.

A

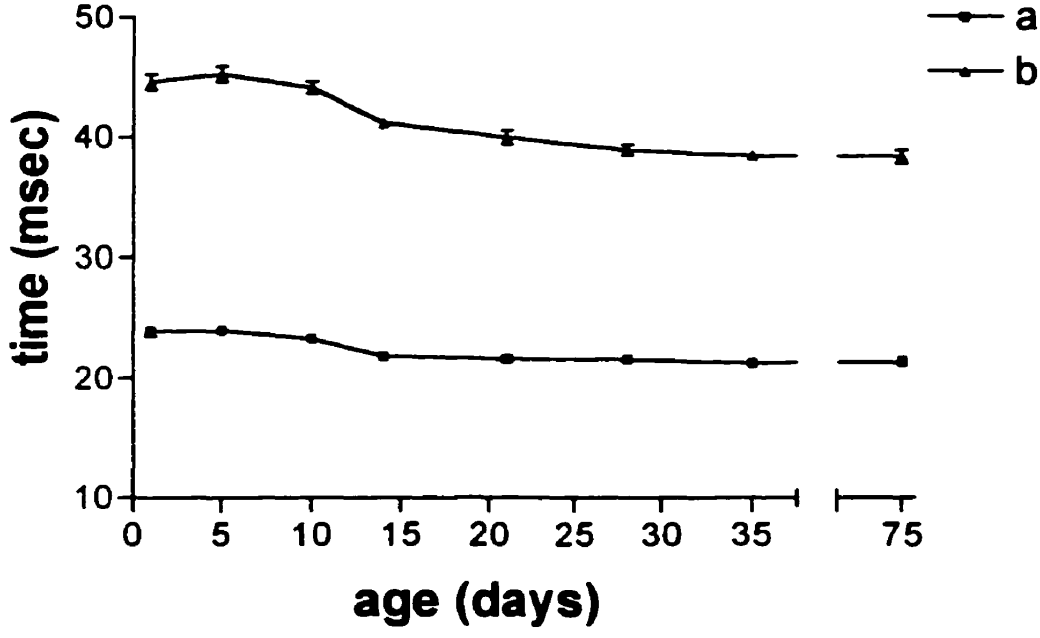
50
40
30
20
10
time (msec)
0
5
10
15
20
25
30
35
75
age (days)
a
b

B

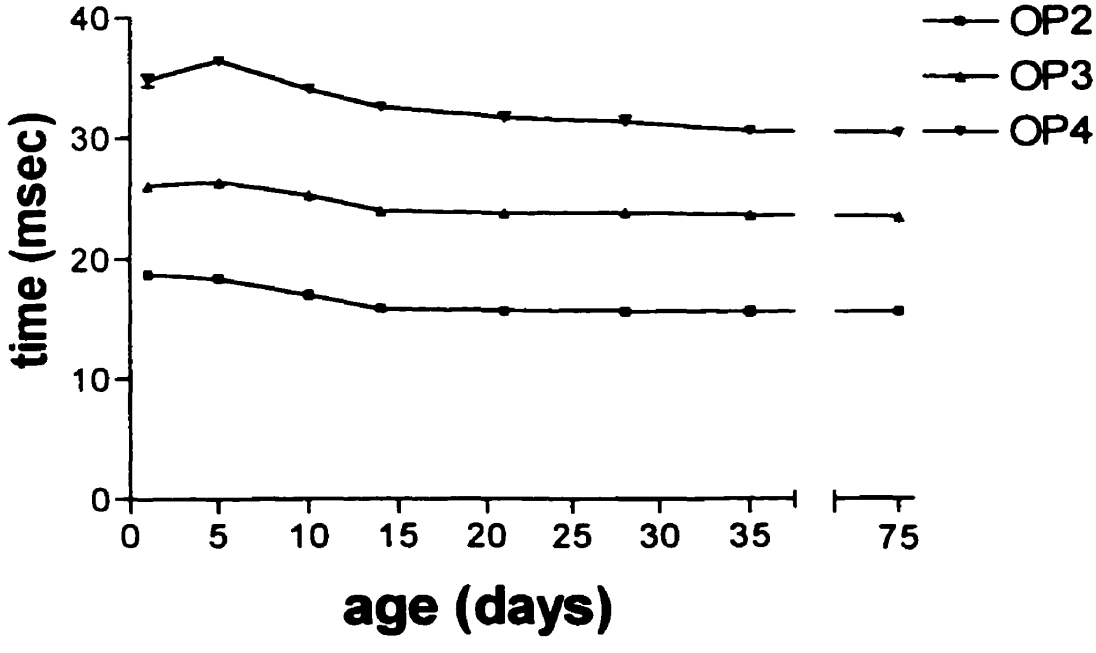
40
30
20
10
0
time (msec)
0
5
10
15
20
25
30
35
75
age (days)
OP2
OP3
OP4

showed a progressive shortening in their timing from P_1 to P_{14}. The timing for all three components remained stable after P_{14}. There was a significant overall decrease ($p<0.05$;$n=11$) in the implicit time between ages P_1 and P_{75} for all scotopic ERG and OP components evoked to a 0.9 log cd.m^{-2}.sec stimulus.

b-wave/a-wave parameters

To examine the b/a-wave ratio in the scotopic intensity response function of the guinea pig, three different stimulus intensities were considered: 0.3 log cd.m^{-2}.sec, -1.2 log cd.m^{-2}.sec, and -1.5 log cd.m^{-2} sec.

The b/a-wave ratio elicited by the three different stimuli and delivered in scotopic conditions are shown in figure 19. A bright stimulus (0.3 log cd.m^{-2} sec) yielded a ratio of approximately 1.00 ± 0.05 at age P_1 (figure 19-A). A similar ratio was observed at age P_5 (1.03 ± 0.11), after which it decreased to age P_{14} (0.65 ± 0.03). The b/a-wave ratio appeared to stabilize after age P_{14}, although there was some variation observed in the ratio with age. A significant decrease ($p<0.05$; $n=11$) was found between the scotopic b/a-wave ratio evoked to a 0.3 log cd.m^{-2}.sec stimulus at ages P_1 and P_{75}.

The b/a-wave ratio evoked to a dimmer stimulus intensity of -1.2 log cd.m^{-2}.sec is shown at figure 19-B. The b/a-wave ratio was shown to increase from 1.20 ± 0.15 at age P_1, to 1.61 ± 0.16 at age P_5. There were only small variations observed in the ratio from ages P_5 to P_{14}. However, there was a decrease in the b/a-wave ratio from ages P_{14} (1.65 ± 0.13) to P_{21} (0.98 ± 0.19), after which the ratio stabilized. There was no significant difference ($p= 0.24$; $n= 11$) between the b/a-wave ratio at ages P_1 and P_{75}.

Figure 19

The effect of aging on the b-wave/a-wave ratio in dark-adapted conditions for three stimuli intensities. The data bars in A (flash intensity = 0.3 log cd. m^{-2} sec), B (flash intensity =-1.2 log cd. m^{-2} sec), and C (flash intensity = -1.5 log cd. m^{-2} sec) represent the mean ± SEM for 11 measurements obtained from 11 guinea pigs.

A

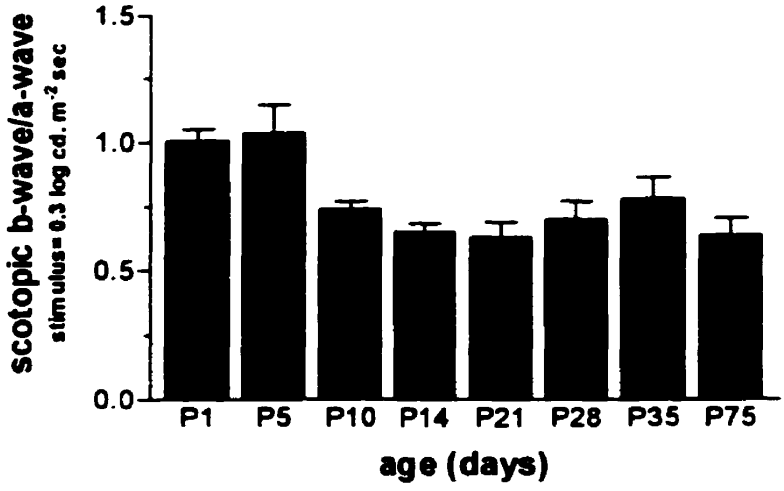
scotopic b-wave/a-wave
stimulus= 0.3 log cd. m-2 sec
1.5
1.0
0.5
0.0
P1
P5
P10
P14
P21
P28
P35
P75
age (days)

B

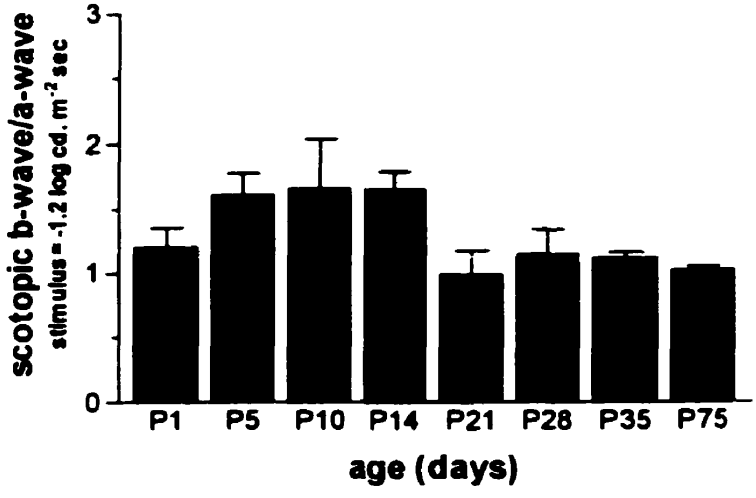
scotopic b-wave/a-wave
stimulus = -1.2 log cd. m-2 sec
3
2
1
0
P1
P5
P10
P14
P21
P28
P35
P75
age (days)

C

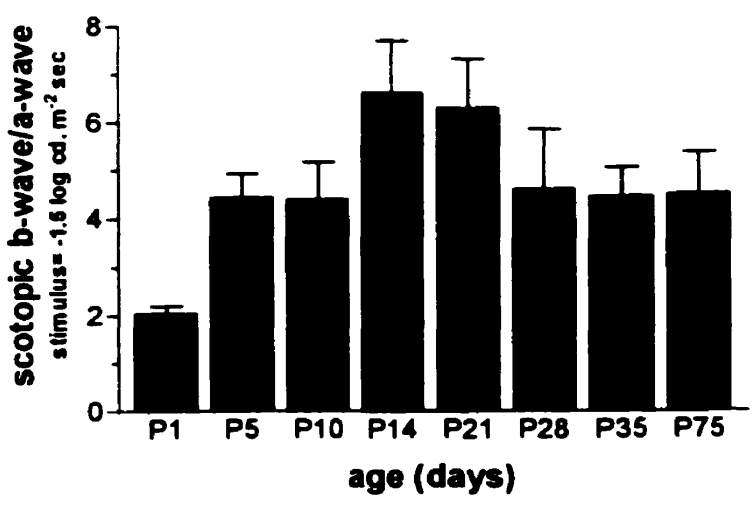
scotopic b-wave/a-wave
stimulus = -1.5 log cd. m-2 sec
8
6
4
2
0
P1
P5
P10
P14
P21
P28
P35
P75
age (days)

A stimulus only 3 log units dimmer in intensity (-1.5 log $cd.m^{-2}.sec$) yielded a much larger b/a-wave ratio (figure 19-C) than the previous example. The b/a-wave more than doubled from age P_1 (2.03 ± 0.16) to age P_5 (4.42 ± 0.50). A further increase in the b/a-wave ratio occurred from ages P_{10} (4.38 ± 0.78) to P_{14} (6.60 ± 1.10). The b/a-wave ratio decreased from P_{14} to age P_{28} (4.60 ± 1.25). After age P_{28}, the b/a-wave ratio remained relatively stable with age. Overall, the b/a-wave ratio evoked to a -1.5 log $cd.m^{-2}.sec$ stimulus showed a significant increase ($p<0.05$; $n=11$) in the amplitudes between the ages P_1 to P_{75}.

Dark adaptation parameters

One of the key features of the guinea pig's dark adapted response was the negitive morphology which is most prominent with bright flashes. We investigated whether this unusual morphology was also present at the onset of dark adaptation. Scotopic ERGs and OPs were recorded within the first minute of dark adaptation from guinea pigs at ages P_{50} to P_{75} that were previously light adapted (background: 30 $cd.m^{-2}$). As shown in figure (20-A), the ERG and OP waveform morphology during the first minute remains relatively unchanged when compared with the ERG morphology of age matched guinea pigs dark adapted for 12 hours (figure 14-A and 14-B). Most notably, there was a negative ERG morphology at a bright flash stimulus. However, as summarized in an intensity-response curve, (figure 20-B) the thresholds and overall amplitudes of the a-wave and b-wave were different than those measured in guinea pigs dark adapted for 12 hours (figure 16-C).

The a-wave threshold measured after 1 minute of dark adaptation was approximately 0.6-log units lower than that measured after 12 hours of dark adaptation, while the amplitude of the a-wave evoked to the brightest flash during the first minute of

Figure 20

Following a period of light adaptation (at least 5 minutes; background: 30 cd. m^{-2}), ERGs (A: left tracing) and OPs (A: right tracings) were simultaneously recorded during the first minute of dark-adaptation for each flash intensity. Flashes spanned over a 6 log-unit range with a maximum flash of 0.9 log.cd.m^{-2} sec. Scotopic intensity-response curves (B) were constructed from the a-wave and b-wave amplitudes recorded at each flash intensity. All data points represent the mean ± SEM for 8 adult guinea pigs. Calibration: horizontal: 10 msec (A and B); vertical 50 μV (left tracings of A) 10 μV (right tracings of B).

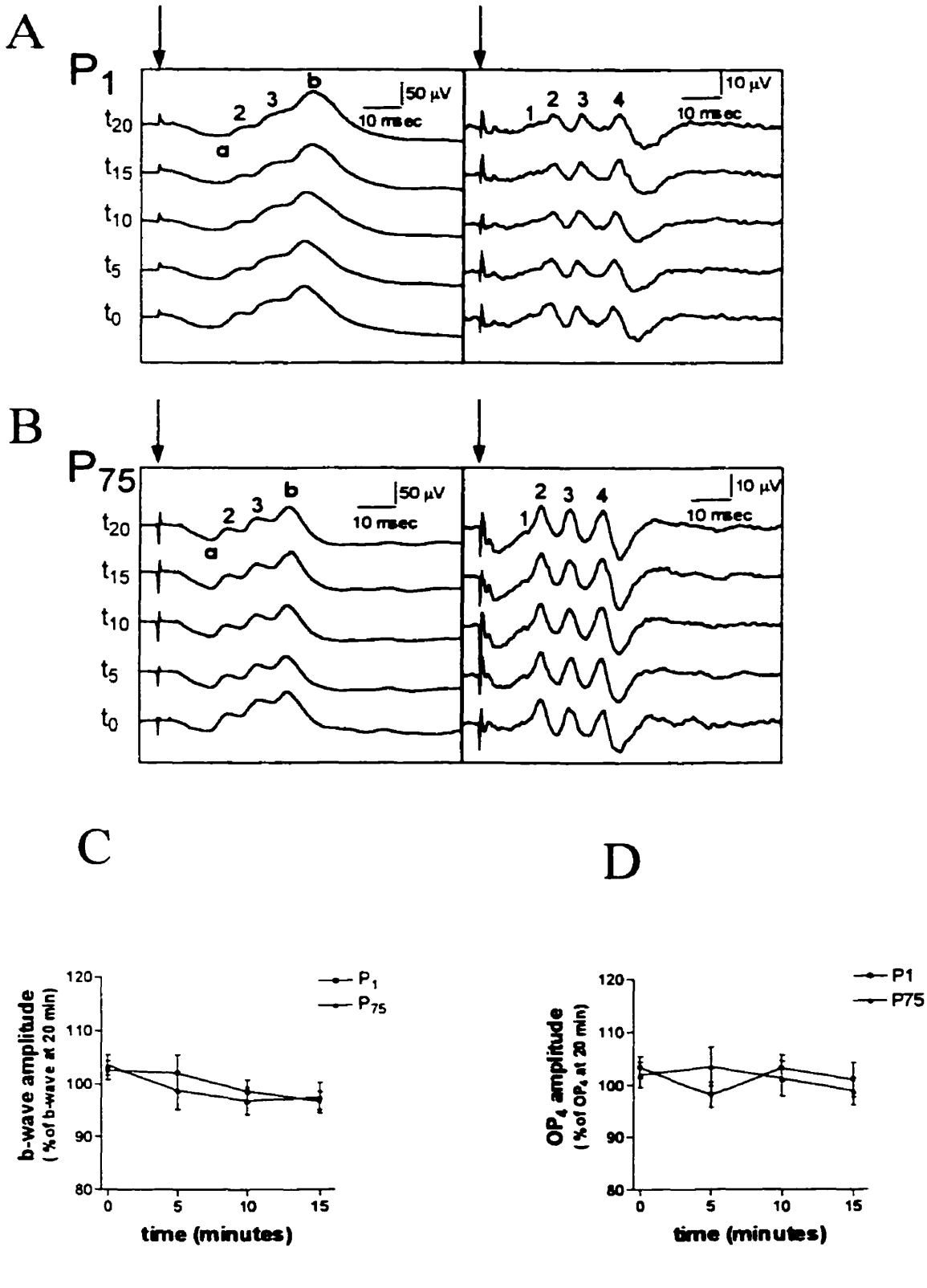
A
P1
t20
t15
t10
t5
t0
a
b
2
3
50 µV
10 msec
1
4
10 µV
B
P75
C
D
b-wave amplitude
(% of b-wave at 20 min)
time (minutes)
P1
P75
OP4 amplitude
(% of OP4 at 20 min)

dark adaptation (85.3 μV ± 7.6 μV) was approximately half the value of that seen after 12 hours of dark adaptation (152.3 μV ± 3.9 μV).

In comparison to that described above, the intensity of stimulation required for the b-wave threshold was about 1.2 log units higher when compared with that measured after 12 hours. The amplitude of the b-wave evoked to the brightest flash during the first minute of dark adaptation (77.2 μV ± 4.5 μV) also displayed a moderate decrease when compared to responses obtained after 12 hours (100.3 μV ± 4.0 μV). Furthermore, the stimulus required to evoke the b-wave threshold during the first minute of dark adaptation was between –3.9 and –2.7 log cd.m^{-2}sec. This stimulus was of notably higher intensities than that required to evoke the b-wave threshold (between –5.1 and –3.9 log cd.m^{-2}sec.) for a guinea pig at age P_{75} dark adapted for 12 hours.

A night blind guinea pig: an unexpected finding

In the course of our experiment, an accidental mating of a brother and sister occurred. Of the four guinea pigs born from this union, one yielded "abnormal" recordings when compared to other guinea pigs. As shown in figure 21-A, a recordable b-wave did not appear until the flash stimulus reached –1.2 log cd.m^{-2} sec. This stimulus was about 2.7 log-units brighter than that required to evoke a threshold b-wave threshold in all the other guinea pigs tested. As the flash stimulus progressively increased to 0.9 log cd.m^{-2} sec, the b-wave amplitude and the implicit time gradually increased. Unlike the responses normally seen in the guinea pig under scotopic conditions, the amplitude of the b-wave displayed no transient reduction in amplitude. The threshold for the a-wave was 0.6 log units higher than the flash energy required to evoke the b-wave threshold, whereas in normals, the a-

Figure 21

The scotopic intensity-response function (A) for the ERG (1-1000 Hz bandwidth) of a guinea pig with unusual dark-adapted recordings. Following a 12 hour period of dark adaptation, this guinea pig was evoked to flashes of white light of increasing flash intensities spanning over a 2.4 log unit range with the maximum flash being 0.9 log.cd.m-^{2} sec. The photopic (background: 30cd.m^{-2}) ERG (B) was evoked to a flash stimulus of 0.9 log.cd.m^{-2} sec. The scotopic intensity-response curve (C) illustrates changes to the a-wave and the b-wave amplitudes with an increasing stimulus intensity. Calibration: horizontal: 20 msec (tracings A and B); vertical 100 μV (tracings A and B).

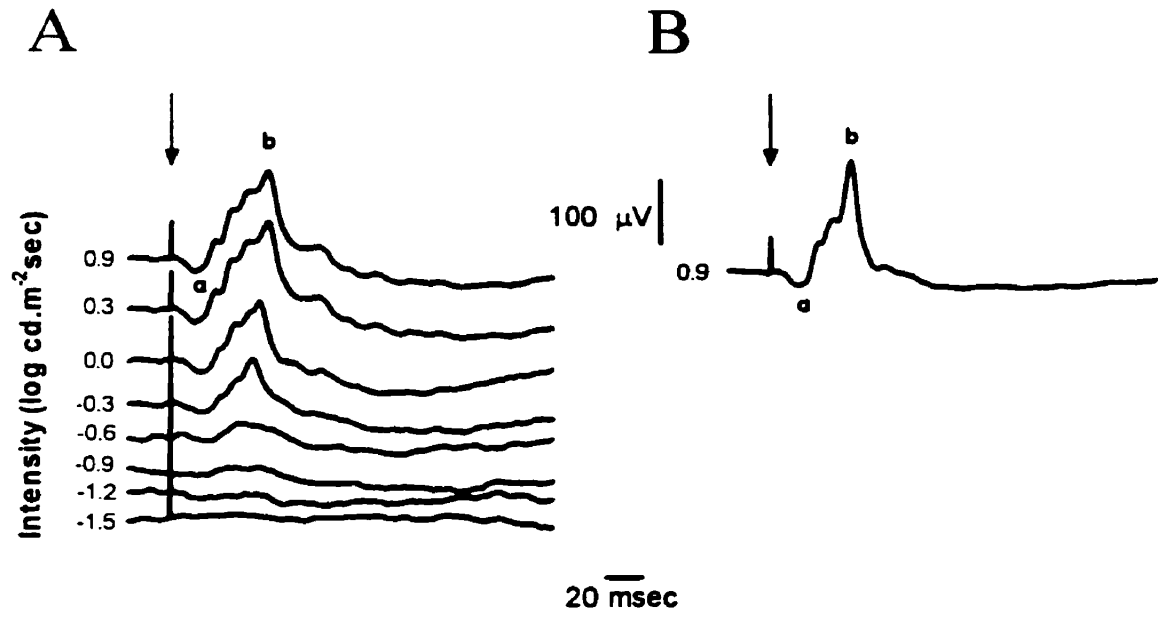
A
B
b
a
0.9
0.3
0.0
-0.3
-0.6
-0.9
-1.2
-1.5
Intensity (log cd.m-2sec)
100 µV
0.9
20 msec

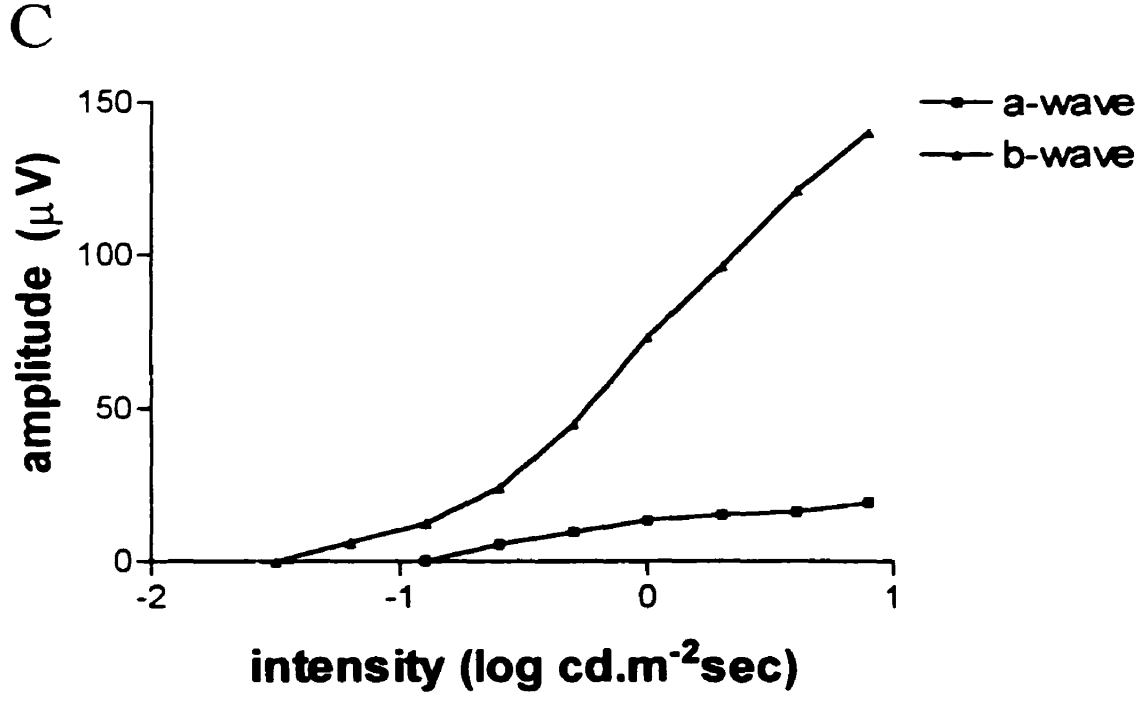
C
150
100
50
0
-2
-1
0
1
amplitude (µV)
intensity (log cd.m-2sec)
a-wave
b-wave

wave can not be recorded until the flash intensity has reached a value approximately 1.5 log units above the b-wave threshold. However, while the a-wave amplitude gradually increased with brighter flashes, its amplitude did not reach the same magnitude as that observed in other normal guinea pigs. As a result, there was no evidence of the negative waveform normally observed in this abnormal guinea pig.

Figure 21-B shows a photopic ERG recorded in response to a bright flash of 0.9 log $cd.m^{-2}$ sec. When compared with the scotopic ERG produced at the same stimulus intensity, the appearance of the photopic a-wave and b-wave amplitudes are about the same. However, the photopic b-wave morphology is distinct as there is one less OP on the ascending limb of the b-wave compared to the b-wave of the scotopic response. Results from the abnormal guinea pig's scotopic ERG are summarized in an intensity-response curve (figure 21-C). As the flash stimulus increased, the scotopic a-wave and b-wave responses of the abnormal guinea pig were profoundly different when compared to the other guinea pigs tested (figure 6-C).

Discussion

Although guinea pigs are born with eyes open and a relatively mature retina, there were significant changes that effected both the photopic and scotopic ERGs/OPs with maturuation.

Photopic responses

The light adapted ERGs and OPs evoked from the neonatal guinea pig not only continue to develop after birth, but the impact of maturation on their development allowed us to distinguish them apart further. More specifically, the b-wave reached its maximum amplitude earlier than the a-wave (P_5 vs P_{10}, respectively: figure 11-A). Strangely, after the b-wave reached its maximum amplitude it rapidly decreased. Abrupt decreases in the ampltiude of the b-wave are not usually seen with the development of the retina. For example, the rabbbit's photopic b-wave was reported to grow linearly during its first 5 weeks of development (Gorfinkel and Lachapelle, 1990). Similarly, the photopic b-wave in humans was reported to progressively increase during its first 8 weeks (Horstein and Winkelman, 1965, Barnet et al., 1965; Breton et al., 1995; Mets et al., 1995).

The overall development of the OPs amplitudes was separate from one another, as well as from the a-and b-waves. Initially, OP_2 and OP_4 reached their maximum amplitude

at P_5 (figure 11-B), whereas OP_3 reached its maximum amplitude at P_{10}. Unlike the amplitude of the a- and b-waves that were stabile at P_{21}, the OPs continued to mature, usually in a complex manner, until P_{75}. El Azazi and Wachtmeister (1991) reported that in rats, the photopic OPs reached maturity at age P_{30}, which is considerably faster development compared to the guinea pig. However, all OPs displayed an overall increase in their amplitudes from ages P_1 to P_{75}, which was similar to other rodents such as the rat (el Azazi and Wachtmeister,1991) and rabbit (Gorfinkel and Lachapelle, 1990).

Gorfinkel and Lachaplle (1990) reported simultaneous development of the b-wave and the OPs for the rabbit and concluded that the developing OPs are important contributors to the developing photopic b-wave. The pattern of photopic maturation was clearly different for the rabbit ERG is compared with that of the guinea pig. The guinea pig's b-wave was stable by P_{21} whereas the amplitudes of the OPs continued to mature until P_{75}. Thus, unlike the rabbit, the Ops of the guinea pig appear to mature distinctly from the b-wave.

Photopic flicker responses

In addition to the developmental differences for each OP mentioned above, the photopic OP responses evoked a flicker stimulus emphasized the individual development of the OPs between and neonatal guinea pigs and guinea pigs at age P_{75}. As the presentation rate of the retinal stimulus is increased, various types of retinal receptors become incapable of responding (Fishman and Sokol, 1990). When OP_3 was evoked to a faster rate of presentation (i.e. 8-16 Hz), the neonatal guinea pigs were unable of produce an OP_3 response. However, as the guinea aged, in more than half of the guinea pigs

analyzed, an obvious OP_3 response could be observed. Obviously, OP_3 matured substantially over this time period. The responses of OP_2 were found to be more resistant to a flicker presentation at 16 Hz than OP_3. OP_2 also showed some maturation as this response became increasingly more resistant to the flicker stimulus with age. Strangely, opposite responses were observed in OP_4: there was a significant decrease observed in the amplitude of OP_4 with age when the guinea pig was presented to a flicker presentation of 16 Hz. Findings from the development of the rat retina using very short inter-stimulus intervals concluded that the generators of the earlier photopic OPs were different compared to the later ones (el Azazi and Wachtmeister; 1991). Similarly in the guinea pig, maturational differences emphasized that the generators of OP_3 and OP_2 were less resistant to a flicker presentation, while OP_4 was more resistant. Changes observed between the amplitude and timing of OP_3 and OP_4 when presented to faster flicker stimulus not only indicates that the mechanism underlying OP_3 and OP_4 are different, but they mature at different rates.

The individual photopic OPs were differentially affected by a flickering stimulus regardless of age. The amplitudes of all the OPs decreased at different rates as the rate of presentation was increased: the amplitude of OP_3 being most affected at a high rate of stimulus presentation and OP_4 being the least affected. Interestingly, the timing of OP_2 was lengthened at a low rate of stimulus presentation, but then shortened as the rate of stimulus presentation was increased. Lachapelle (1991) reported that a flicker presentation evoked to humans' showed that each OP represents an independent electrophysiological entity. The data presented in this study for the developing retina of the guinea pig would support this claim 2 ways: 1) the developmental differences between each OP was unique;

and, 2) the changes to the amplitude and peak time of each OP, regardless of age, was independent from one another.

It is also interesting to note that the photopic flicker responses of the guinea pig are similar to that of humans evoked to the same stimuli (Nagata, 1963; Kojima and Zrenner, 1978; Lachapelle, 1991). In humans, a flicker presentation of 10 Hz reduced the amplitudes of OP_2 and OP_3 with increasing flicker rate, whereas the amplitude of OP_4 was reduced. Furthermore, the peak time of OP_2 was increased, whereas the peak time of OP_4 was reduced. In guinea pigs, a flicker presentation of 8 Hz or 16 Hz produced similar results as those mentioned above with the exception that the amplitude of OP_4 is reduced as the flicker rate increases. With this exception to OP_4, both guinea pigs and humans show similar physiological differences between the photopic OPs when evoked to a slow flicker stimulus and therefore, the guinea pig might represent an excellent model to investigate the mechanisms that underlie these responses. Determining the mechanisms of how the retina reacts to a flicker presentation might help us to understand the pathology of an acquired cone dystrophy.

Interpreting the light adaptation effect

The light adaptation effect recorded from guinea pigs at ages P_1 and P_{75} (figure 16) was interesting for two reasons. First, there was no difference found between these two age groups for light adaptation effects, although all photopic ERG components displayed significant maturational changes. Benoit et al. (1994) reported that the LAE was not usually observed in the infant rat, although this response was notably apparent in adult rats. The failure of the LAE to appear in the guinea pig demonstrates that this retinal

element did not mature in the rat. Second, all guinea pigs failed to display the LAE as was also reported for the rat. Normally, in humans (Lachapelle, 1987; Gouras and Mackay, 1989; Peachey et al., 1989) and rodents (Peachey et al. 1993, Benoit et al., 1994), the LAE identifies the phenomenon whereby the amplitude of the cone b-wave increases for approximately 10 minutes, following a period of dark adaptation. Since the majority of the LAE is observed in the b-wave and OP4, it has been suggested that this effect is generated postreceptorally (Lachapelle, 1987; Gouras and Mackay, 1989; Peachey et al., 1989b; Koichiro and Sieving, 1992). While the exact origin of the LAE is still unknown, it has been reported to be highly dependent upon the intensity of the flash stimulus (Armington and Biersdorf, 1958; Gouras and Mackay, 1989; Peachey et al., 1989b). Why does the retina of the guinea pig not require time to adapt from a scotopic environment to a photopic one? Koichiro and Sieving (1992) considered the b-wave growth of the LAE might result from a change in the balance of the depolarizing ON-bipolar cells and the hyperpolarizing OFF-bipolar cells. If the "push/pull" model generates the b-wave as suggested by Sieving et al. (1994), then hyperpolarizing OFF-bipolar cells may restrict the growth of the b-wave. The guinea pig has been reported to have 8-17% (Peichl and Gonzalez-Suriano, 1994) cones whereas humans have 5% (Curcio et al., 1990), and rats have 1% (Szel and Rohlich, 1992) cones. One wonders whether a larger percentage of cones in the guinea pig could modify the relative balance of the of the depolarizing pathway vs the hyperpolarizing pathway and account for these unusual results. If the hyperpolarizing OFF-bipolar cells do govern the LAE, then increasing the input to the depolarizing ON-bipolar cells might overcome this restriction, and result in a loss of the LAE.

Scotopic responses

The scotopic ERG obtained from the developing retina of the guinea pig are clearly different from that observed in other species, including rodents. The complexity of this maturation is best depicted at figure 14. As reported for most species, a shortened peak-time and increased amplitude marks the maturation of the scotopic a-wave and b-wave. This was observed for the maturing a-wave of the guinea pig from ages P_1 to P_{14}. In contrast, a different picture emerged for the dark-adapted b-wave evoked to bright flashes. The b-wave amplitude reached a maximum at age P_5 and then decreased with age. However, there was still a shortening of the implicit time observed with the b-wave. The changes observed with the development of the scotopic b-wave are inconsistent with that reported in other species (e.g. the cat: Zetterstrom, 1955; the rabbit: Noell, 1958; Gorfinkel, 1988; the dog: Gum et al., 1973; the rat: Braekevelt and Hollenberg, 1970; el Azazi and Wachtmesiter, 1990). Furthermore, the a-wave, b-wave, and OPs all reached their maximal amplitudes at a different postnatal age (figure 17). Given that the postnatal pattern of development of the scotopic oscillatory peaks differed form that of the a- and b-waves, and there was also an individual development of the OPs, our results are in accordance with other studies which suggested that these components come from independent origins (Wachtmeister 1972, 1980; Wachtmeister and Dowling, 1978; Heynen et al., 1985).

In the present study, the photopic and scotopic a- and b-waves developed concurrently. The peak time and amplitudes of both components were stabile at age P_{21}. This is in concert with Huang et al. (1990) who reported that during the initial stages of

retinal development *in utero*, the scotopic and photopic components of the guinea pig's ERG developed at the same rate. However, in the present study, it was also interesting to observe that the amplitude of the scotopic OPs stabilized at P_{28}, whereas the photopic OPs continued to develop at least until age P_{75}. Thus, the scotopic OPs mechanism underlying the OPs seemed to develop faster than the photopic system involved in the generation of the OPs. Previous studies have also reported in the developmental difference in the photopic and scotopic systems. El Azazi and Wachtmeister (1990) reported that in rats, the scotopic mechanisms underlying the OPs seemed to mature faster than the photopic system. However, the scotopic system does not always develop faster. For example, Hortstein and Winkelman (1965) showed that in human infants, the photopic components reaches maturity at 2 months after birth, whereas dark adapted ERGs gradually reached adult levels at approximately one year. The reason for one system to develop faster than the other remains unknown.

At the beginning of this study, we hypothesized that there might be a connection between the percentage of cones in the retina and which visual system develops faster. For example, the retina of the rat, which is is a nocturnal animal, consists of about 1% cones and their scotopic system develops more quickly than the photopic system. Conversely, in humans with approximately 5% cones and a more diurnal behavior, the photopic system develops more quickly than the scotopic one. However, as reported above, the guinea pig has 8-17% cones and a diurnal behavior, possesses a scotopic system thatdevelops faster than its photopic system. As demonstrated in this study, the percentage of cones in the retina did not appear to determine whether the scotopic or photopic rate was first to mature. The factor(s) that govern which visual system develops first remains unresolved.

As shown above, both photopic and scotopic systems demonstrate postnatal maturation. However, do all ERG componets, and consequently the retinal structured at their origin, show a similar maturation? Shortly after birth the scotopic and photopic b-waves reached maximum amplitudes before respective a-waves. Also after birth, the b-wave/a-wave ratio was at higher values compared to the ratios at age P_{75}. These results can only be explained if elements of the b-wave mechanism (inner retina) are more mature than those of the a-wave (outer retina). This claim is supported by early histological results (Huang et al., 1990) in guinea pigs that the inner retinal structures develop before the outer segments of the photoreceptors. Furthermore, our results show that b-wave/a-wave ratio decreases with age as one would expect if the inner retina matures before the outer retina. However, as mentioned in the introduction, the mechanisms responsible for the generation of the OPs are thought to be at the level of the inner retina. The OPs development appears to mature after the a-wave, especially in photopic conditions. Thus, specific sections of the inner retina may mature faster (i.e. mechanism underlying the b-wave) than the outer retina (i.e. mechanisms underlying the a-wave), but continue to mature (i.e. the mechanisms underlying the OPs) after the outer retina has matured.

Another point of interest is that when compared with other rodents, such as the rat (figure 4), the scotopic intensity response function obtained from the guinea pig is strikingly different. Progressively brighter flashes evoked to the rat lead to ERG components with greater amplitudes. Similar changes were noticed in the scotopic intensity response function of the guinea pigs, but only when evoked to dimmer stimuli. However, with brighter flashes, the scotopic ERG of the guinea pig became negative as

was recently shown (Bui et al., 1998; Bui et al., in press). The negative morphology observed in the guinea pig at bright flashes is not seen in other rodents or any other animal to our knowledge.

What could cause the negative waveform morphology displayed in the scotopic b-wave? A possible answer began to reveal itself with the discovery of an abnormal guinea pig that was labeled "night blind" because it appeared to have no rod function, but a normal cone function. This night blind guinea pig did not produce a negative scotopic ERG at bright flash intensities but rather produced a waveform almost identical to that seen in photopic conditions. Thus, the negative morphology normally produced at a bright flash intensity could be the result of a scotopic system and photopic system interaction. As previously mentioned, the guinea pig has been reported to have 8-17% cones (Peichl and Gonzalez-Suriano, 1994), a percentage much larger than humans or rats. Furthermore, in humans, normally the b-wave implicit time for the photopic system (26-34 msec) is much faster than the scotopic system (40-56 msec)(Fishman and Sokol, 1990). However, the guinea pig's photopic b-wave implicit time (38-43 msec) is only slightly faster than the scotopic b-wave implicit time (40-45 msec). Since the implicit timing of the b-wave for these two systems are quite similar, the hyperpolarizing OFF-bipolar cell activity of the photopic b-wave (descending limb) might overlap with the depolarizing ON-bipolar cells of the scotopic b-wave (ascending limb) at bright flashes. Thus, the negative waveform morphology could be the result of a postreceptoral cone inhibition of rod mediated activity, which would be significantly more powerful in guinea pigs because of an increased percentage of cones and/or an overlapping of the descending limb of the photopic b-wave with the ascending limb of the scotopic b-wave.

The results obtained from the first minute of dark adaptation are not in complete agreement with the above argument. As mentioned in the introduction, there are significant adaptive changes observed in the ERG upon the onset of dark adaptation following a period of light adaptation. The guinea pig did show an increased threshold for the b-wave and an overall decrease in the maximum amplitude obtained for the ERG components compared with guinea pigs dark adapted for 12 hours (figure 14 and figure 16). However, the negative morphology reported to occur after 12 hours of dark adaptation was equally apparent during the first minute of dark adaptation. If the negative morphology was caused by a rod-cone interaction, one might suspect that the negative morphology would become more prominent as the regeneration of rhodopsin was achieved. Changes normally expected during the first minute of dark adaptation to the rod-cone contribution to the ERG evoked do not appear to influence the negative morphology unique to the guinea pig. Whether the mechanism governing the negative morphology is the result of a rod-cone interaction remains undetermined. A subject for a future investigation might use APB to selectively block the activity of the ON-bipolar cells (Slaughter and Miller, 1981; Neil et al., 1981; Arkin and Miller, 1987) and PDA to selectively block the activity of the OFF-bipolar cell (Slaughter and Miller, 1983a,b; Dvorak, 1984), in order to resolve the mechanism(s) which might be involved.

Histological evidence also showed that the normal guinea pig has unusually large horizontal cells when compared with other rodents (Dassa et al., 1998). Horizontal cells mediate lateral interactions, although their detailed retinal processing in unknown (Wassle and Boycotte, 1991). When stimulated, these horizontal cells may modify the evoked potential that stimulates the bipolar cells and results in negative ERGs. Normally however,

dysfunction of cells within the inner nuclear layer can selectively decrease the ERG b-wave amplitude without diminishing the ERG a-wave. Since the scotopic a-wave is reamkedly reduced, it is most likely that the retinal disorder affecting the night blind guinea pig occurs at the level of the rod photoreceptor. Whether the absence of a normal scotopic response results from an abnormality of the rod photoreceptor and/or an absence of horizontal cells remains to be determined through histological examination. Further investigations involving this "special" night blind guinea pig requires additional off-spring with similar retinal function. Only after additional night blind guinea pigs are born can the evaluation of the retinal histology be performed. The breeding of this night blind guinea pig is presently underway.

CONCLUSIONS

- This study clearly demonstrates that retinal development of the guinea pig continues after birth.

- The amplitude of the OPs were the last ERG components to mature: the scotopic OPs matured faster than the photopic OPs. Consequently, it was determined that the scotopic system matures faster than the photopic system. This result was similar to the studies investigating the development of the rat retina and contrasts with studies investigating the retinal development of humans

- Results from both the photopic and scotopic system showed that the b-wave was the first ERG component to reach its maximum amplitude, followed by the a-wave. The photopic and scotopic b-wave/a-wave ratio also decreased in the guinea pig with age. Histological evidence from a previous study and the above results suggest that specific elements of the inner retina (the mechanisms underlying the b-wave response) mature before the outer retina (the mechanisms underlying the a-wave response).

-The light adaptation effect, which is normally observed in most animals, was not observed in the guinea pig and therefore no maturation of this element could be observed. It was hypothesized that an large percentage of cones compared with other animals might account for the loss of this effect.

-It was shown using a slow flickering stimulus of 16 Hz that OP_4 was the most resistant while OP3 was the least resistant. Furthermore, OP3 and OP2 matured to become more resistant to a 16 Hz flicker presentation with age. while that of OP4 was appear to be relatively mature and resistant at birth.

-The individual development of each OP in this animal study supports previous human studies concluding that each OP represents an independent electrophysiological entity.

- The scotopic ERG was unique in that at bright flashes produced a negative morphology not observed in any other normal animal to our knowledge. It was hypothesized that the mechanism underlying this response could be the result of a photopic-scotopic interaction based on the "push/pull" model of the b-wave. A night blind guinea pig was discovered, evaluated, and the results are in accord with this hypothesis.

References

Armington, JC, & Biersdorf, WR (1958). Long term light adaptation of the human electroretinogram. *J Comp Physiol* 51: 1-5.

Arkin, M, & Miller, R (1987). Subtle actions of 2-amino,4-phosphonobutyric acid (APB) on the off pathways in the mudpuppy retina. *Brain Res* 23: 1615-1620.

Barnet, AB, Lodge, & Armington, JC (1965). Electroretinogram in newborn human infants. *Science* 148: 651-654.

Benoit, J, & Lachapelle, P (1995). Light adaptation of the human photopic oscillatory potentials: influence of the length of the dark adaptation period. *Doc Ophthalmol* 89: 267-276.

Benoit, J, Lachapelle P, McKerral M, Tremblay I, Jutras S, & Molotchnikoff S (1994). Unusual light adaptation effect in rats. *Invest Ophthalmol Vis Sci (suppl)* 35: 2046.

Bornschein, H (1959). Zur postnatalen entwicklung der netzhautfunktion. *Wein KlimWochen* 49: 956-958.

Braekevelt, C, & Hollenberg, M (1970). The development of the retina of the albino rat. *Am J Anat* 127: 281-302.

Breton, ME, Quinn, GE, & Schueller, AW (1995). Development of the electroretinogram and rod phototransduction response in human infants. *Invest Opthalmol Vis Sci* 36: 1588-1602.

Brindley, GS (1956). Responses to illumination recorded by microelectrodes from the frog's retina. *J Physiol (Lond)* 134: 360.

Brindley, GS (1957). The passive electrical properties of the retina and the sources of the electroretinogram. *Bibl Ophthalmol* 48: 24-31.

Brown, & KT (1968). The electroretinogram: its components and their origins. Vision Res. 8: 633-677.

Brown, KT, & Wiesel, TN (1961). Analysis of the intraretinal electroretinogram in the intact cat eye. *J Physiol (Lond)* 158: 229-256.

Brown, KT, & Wiesel, TN (1961). Localization of origins of electroretinogram components by intraretinal recording in the intact cat eye. *J Physiol (Lond)* 158: 257-280.

Brunette, JR, & Desrochers, R (1970). Oscillatory potentials: a clinical study in diabetics. *Can J Ophthalmol* 5: 373-380.

Bui, BG, Sinclair, AJ, & Vingrys, AJ (1998). Electroretinogrmas of albino and pigmented guinea pigs (Cavia Porcellus). *Australian and New Zealand J Opthalmol* 26: S98-S100.

Bui, BG, Weisinger, HS, Sinclair, AJ, & Vingrys, AJ (in press). Comparison of Guinea pig electroretinograms measured with bipolar corneal and unipolar intravitreal electrodes. *Doc Ophthalmol.*

Burian, HM (1954). Electric responses of the human visual system. *Arch Ophthalmol* 52: 509-24.

Burian, HM, & Allen, LA (1954). A speculum contact lens electrode for electroretinography. *Electroenceph Clin Neurophysiol* 6: 509-511.

Bush, R, & Sieving, P (1994). A proximal retinal component in the primate ERG a-wave. *Invest Opthalmol Vis Sci* 35: 635-645.

Cobb, WA, & Morton HB (1954). A new component of the human electroretinogram. *J Physiol* 123: 36-37.

Curcio, C, Sloan, K, Kalina, R, & Hendrickson, A (1990). Human photoreceptor topography. *J of Comp Neurolology* 292: 497-523.

Dassa, J, Behn, D, Cassanova, C, & Lachapelle, P (1998). Maturation of the oscillatory potentials gradually shapes the unique morphology of the guinea pig's ERG. *Invest Ophthalmpol Vis Sci* 39 (suppl): 864.

Dawson, W, Trick, G, & Litzkow, C (1979). Improved electrode for electroretinography. *Invest Ophthalmol Vis Sci* 18: 988-991.

DeMolfelta, V, Spinellei, M, & Polengi, F (1968). Behavior of the electroretinographic oscillatory potentials during adaptation of darkness. *Arch Ophthalmol* 79: 531-535.

Dewar, J (1877). The physiological action of light. *Nature* 15: 433-435.

Dick, E, Miller, RF, & Bloomfield, S (1985). Extracellular K activity changes related to electroretinogram components of Rabbit (E-type) retinas. *J Gen Physio* 85: 911-931.

Dowling, JE (1970). Organization of vertebrate retinas. *Invest Ophthalmol* 9: 655.

Dvorak, D (1984). Off pathway synaptic transmission in the outer retina of the axolotl is mediated by a kainic acid-preferring receptor. *Neurosci Lett* 50(1-3): 7-1 l.

el Azazi, M, & Wachtmeister, L (1990). The postnatal development of the oscillatory potentials of the electroretinogram: Basic characteristics. *Acta Ophthalmologica* 68: 401- 409.

el Azazi, M, & Wachtmeister, L (1991). The postnatal development of the oscillatory potentials of the electroretinogram II: Photopic characteristics. *Acta Ophthalmologica* 69: 6-10.

Fishman, G, & Sokol, S (1990). Components and origins of the ERG. In: Fishman, G and Sokol, S ed. Electrophysiological Testing in disorders of the retina, optic nerve, and visual pathway. Singapore: Palace Press La Jolla: 8-20.

Gofinkel, J, Lachapelle, P, & Molotchnikoff, S (1988). Maturation of the electroretinogram of the neonatal rabbit. *Doc Ophthalmol* 69: 237-245.

Gofinkel, J, & Lachapelle, P (1990). Maturation of the photopic b-wave and oscillatory potentials of the electroretinogram of the neonatal rabbit. *Can J Ophthalmol* 25 (3): 138-144.

Gouras, P, & Mackay, C (1989). Growth in amplitude of the human cone electroretinogram with light adaptation. *Invest Ophthalmol Vis Sci* 30: 625-630.

Granit, R (1933). The components of the retinal action potential and their relation to the discharge in the optic nerve. *J Physiol* 37: 283-307.

Granit, R (1962). The visual pathway. *The Eye* 2: 537- 691.

Graur, D, Hide, W, & Li, W. (1991) Is the guinea pig a rodent? *Nature* 351: 649-652.

Guité, P, & Lachapelle, P (1990). The effect of 2-amino-4-phosphonobutyric acid on the oscillatory potentials of the electroretinogram. *Doc Ophthalmol*, 75: 125-133.

Gum, G, Gelatt, K, & Samual, D (1973). Maturation of the retina of the canine neonate as determined by electrophysiology and histology. *Am J Vet Res* 45(6): 1166-1171.

Hamasaki, DI, & Maguire, GW (1985). Physiological development of the kitten's retina: an electroretinographic study. *Vision Res* 25(11): 1537-1543.

Hanitzsch, R, Lichtenberger, T, & Mittig, W (I 996). The influence Of $MgCI_2$ and APB on the light induced potassium changes and the ERG b-wave of the isolated superfused rat retina. *Vision Res* 36: 499-507.

Henkes, H (1951). Use of electroret-inography in measuring the effects of vasodilatation. *Angiology* 2:125.

Hebert, M, Lachapelle, P, & Dumont, M (1996). Reproducibility of electroetinograms recorded with the DTL electrodes. *Doc Ophthalmol* 91: 333-342.

Heynen, H, & van Norren, D (1985). Origin of the electroretinogram in the intact macaque eye. Principal component analysis. *Vision Res* 25: 697-707.

Heynen, H, Wachtmeister, L, & van Norren, D (1985). Origin of the oscillatory potentials in the primate retina. *Vision Res* 25: 1365-1373.

Holmgren, F (1865). En method att objektivera effekten av zjusintryck pi retina. *Ups Liikaref Forh* 1: 177-191.

Hood, DC, & Birch, DG (1990a). A quantitative measure of the electrical activity of human rod photoreceptors using electroretinography. *Visual Neurosci* 5: 379-387.

Hood, DC, & Birch, DG (1990b). The a-wave of the human electroretinogram and rod receptor function. *Invest Ophthalmol Vis Sci* 31: 2070-2081.

Hood, DC, & Birch, DG (1993). Human cone receptor activity: the leading edge of the a-wave and models of receptor activity. *Visual Neurosci* 10: 857-871.

Hood, DC, & Birch, DG (1995). Phototransduction in human cones measured using the a-wave of the ERG. *Vision Res* 35: 2801-2810.

Hortstein, GP, & Winkelman, JE (1965). The electric activity of the eye in the first days of life. *Acta Physiolo Pharmacol Neerl* 13: 1.

Huang, J, Wyse, J, & Spira (1990). Ontogenesis of the electroretmogram in a precocial mammal, the guinea pig (Cavia porcellus). *Comp Biochem Physiol* 95(1): 149-155.

Ikeda, H, & Jacobson, S (1982). Cone and rod electroretingrams during development in the cat. *J Physiol Lond* 329: 21.

Jacobs, G, & Deegan, J (1994). Spectral sensitivity, photopigments, and color vision in the guinea pig (cavia porcellus). Behav Neurosci. 108(5): 993-1004.

Karpe, G (1945). The basis of clinical electroretinography. *Acta Ophthalmol (Suppl)* 24: 1-118.

King-Smith, P, Loffing, D, & Jones, R (1986). Rod and cone ERGs and their oscillatory potentials. *Invest Ophthalmod Vis Sci* 27: 270-273.

Kirk, G, & Boyer, S (1973). Maturation ofthe electroretinogram in the dog. *Experimental Neurology* 38: 252-264.

Koichiro, M, & Sieving, P (1992). Different rates of growth of monkey and human photopic a-, b-, and d-waves suggest two sites of ERG light adaptation. *Clin Vision Sci* 7(5): 385-392.

Kojima, M, & Zrenner, E (1978). OFF components in response to brief light flashes in the oscillatory potentials of the human electroretinogram. *Albrecht to Graefes Arvhiv fur Klinische Experimetelle Opthalmologie* 206: 107-120.

Kurihara, H (1977). Developmental process of ERG of the albino rat. *Jpn J Ophthalmology* 81:1313-1320.

Li, W, Hide,W, Zharkikh, A, Ma, D, & Graur, D (1992). The molecular taxonomy and evolution of the guinea pig. *J. Heredity* 83: 174-181.

Lachapelle, P, Benoit, J, Blain, L, Guite, P, & Roy, M (1990). The oscillatory potentials in response to stimuli of photopic intensities delivered in dark adaptation: an explanation or the conditioning effect. *Vis Res* 30: 503-513.

Lachapelle, P, Benoit J, Little J, & Lachapelle B (1993). Recording the oscillatory potentials with the DTL electrode. *Doc Ophthalmol* 83:1 19-130.

Lachapelle, P, & Molotchnikoff, S (1986a). Components of the electroretinogram: a reappraisal. *Doc Ophthalmol* 63: 337-348.

Lachapelle, P, & Molotchnikoff, S (1986b). A composite nature for the photopic bwave of the human electroretinogram as evidenced by the use of the 60 Hz notch filter. *Can J Ophthalmol* 21 (1): 19-22.

Lachapelle, P, Little, J, & Polomeno, R (1983). The photopic electroretinogram in congenital stationary night blindness with myopia. *Invest Ophthalmol Vis Sci* 24: 442-450.24: 442-450.

Legein, C, & van Hof, M (1970). The effect of light deprivation on the electroretinogram of the guinea pig. *Pflugers Arch Ges Physiol* 318: 1-6.

Marmor, M, Arden, G, Nilsson, SE, & Zrenner, E (1989). Standard for clinical electroretinography. *Arch Ophthalmol* 107: 816-819.

Mets MB, Smith, VC, Pokorny, J, & Pass, A (1995). Postnatal development as measuremd by the electroretinogram in premature infants. *Doc Opthalmol* 90:111-127.

McKerral, M, Rousseau, S, Lachapelle, P, & Goyal, S (1995). Evidence suggesting that the i-wave of the flash ERG is equivalent to the b-wave of the pattern ERG. *Invest Ophthalmol Vis Sci (suppl)* 36: 449.

Miller, RF, & Dowling, JE (I 970). Intracellular responses of the Müller (glial) cells of mudpuppy retina: their relation to b-wave of the electroretinogram. *J Neurophysiol* 33: 323-341.

Miyake, Y, Horiguchi, M, Ota, I, & Takabayashi, A (1987). Characteristic ERG flicker anomaly in incomplete congenital stationary night blindness. *Invest Ophthalmol Vis Sci* 28: 1816-1823.

Miyake,Y, Horiguchi, M, Ota, I, & Takabayashi, A (1988). Adaptational change in cone mediated electroretinogram in human and carp. *Neurosti Res (Suppl)* 8: 13.

Nagata, M (1963). Studies on the photopic ERG of the human retina. *Jpn J Ophthalmol* 7: 96-124.

Narfstrom, K, Ivert, L, Anderson, BE, & Gouras, P (1993). Light adaptation of the cat cone ERG. *Invest Ophthalmol Vis Sci* (Suppl) 34: 1272.

Neil, M, Cunnigham, J, James, T, Joseph, M, & Collins, J (1981). The effect of 2-amino,4-phosphonobutyric acid (APB) on acetylcholine release from the rabbit retin: evidence for on channel input to cholinergic amacrine cell: *Neurosci Lett* 26: 301-305.

Newman, EA (1980). Current source density analysis of the b-wave of the frog retina. *J Neurophysiol* 43: 1355-1366.

Newman, EA, & Odette, LL (1984). Model of electroretinogram b-wave generation: a test of the K+ hypothesis. *J Neurophysiol* 51: 164-182.

Noell, W (1954). The origin of the electroretinogram. *Am J Ophthalmol* 38: 78-90.

Noell, W (1958). Studies on visual cell variability and differentiation. *Ann NY Acad Sci* 74:337-361.

Ogden, TE (1973). The oscillatory waves of the primate electroretinogram. *Vision Res* 13: 1059-1074.

Peachey, N, Alexander, R, & Fishman, G (1987). Rod and cone system contributions to ocsillatory potentials: an explanation for the conditioning effect. *Vision Res* 27: 859-866.

Peachey, N, Alexander, K, & Fishman, G (1989a). The luminance-response function of the dark-adapted human electroretinogram. *Vison Res* 29(3): 263-270.

Peachey, N, Alxexander, K, Fishman, G, & Derlack, D (1989b). Properties of the human cone system electroretinogram during light adaptation. *Applied Optics* 28: 1145-1150.

Peachey, N, Goto, Y, Al-Ubaidi, M, & Naash, M (1993). Properties of the mouse cone-mediated electroretinogram during light adaptation. *Neuroscience Lett* 162: 9-11.

Peichl, L, & Gonzalez-Suriano, J (1994). Morphological types of horizontal cells in rodent retinae: A comparison of rat, mouse, gerbil, and guinea pig. *Visual Neuroscience* 11: 501-517.

Penn, RD, & Hagins, WA (1969). Signal transmission along retinal rods and the origin of the electroretinographic a-wave. *Nature*. 223: 201-205.

Rousseau, S, McKerral, M, & Lachapelle, P (1996). The i-wave: Bridging flash and pattern electroretinography. *Functional Neuroscience (EEG suppl.)* 46: 167-173.

Sanada, T (1962). Study on the ERG on suckling rabbits. Report I. Development of the ERG (in dark adaptation). *Jpn J Ophthalmol* 66: 1430-1436.

Schneider, T, Olsen, B, & Zrenner, E. (1986) Characteristics of the rod-cone transition in electroreinograms and optic nerve response. *Clin Vision Sci* 1: 81-91.

Sempl S, & Dawson, W. (1987) Retinal cyclic light damage threshold for albino rats. *Laboratory Animal Science* 37: 289-298.

Shipley, T, & Anton, M (1964). The human electroretinogram in the first day of life. *J Ped* 65: 733-739.

Sieving, P, Murayama, K, & Naarendorp, F (I 994). Push-pull model of the primate photopic electroretinogram: a role for hyperpolarizing neurons in shaping the b-wave. *Visual Neurosci* 11: 519-532.

Slaughter, M, & Miller, R (1981). 2-amino, 4-phosphonobutyric acid: a new pharmocological tool for retina research. *Science* 211: 182-184.

Slaughter, M, & Miller, R (1983a). An excitatory amino acid antagonist blocks cone input to sign-conserving second-order retinal neurons. *Science* 219(4589): 1230-1232.

Slaughter, M, & Miller, R (1983b). Bipolar cells in the mudpuppy retina use an excitatory amino acid neurotransmitter. *Nature* 303(5917): 537-538

Speros, P, & Price, J (1981). Oscillatory potentials: history, techniques and potential use in the evaluation of disturbances of retinal circulation. *Surv Ophthalmol* 251: 237-252.

Stockton, RA, & Slaughter, MM (1989). b-wave of the electroretinogram, a reflection of ON bipolar cell activity. *J Gen Physiol* 93: 101-122.

Szel, A, & Rohlich, P (1992). Two cone types of rat retina detected by anti-visual pigment antibodies. *Exp Eye Res* S5: 47-52.

Tian, N, & Slaughter, MM (1994). Correlation of dynamic responses in the ON bipolar neuron and the b-wave of the electroretinogram. *Vision Res.* 35: 9-13.

Tomita, T, & Torihama, Y (1956). Further study on the intraretinal action potentials on the site of ERG generation. *Jpn J Physiol* 6:118-136.

Tomita, T (1963). Electrical activity in the vertebrate retina. *J Opt Soc Am* 53: 49-57.

Tsuchida, Y, Kawasaki, K, Fujimura, K, & Jacobson, JH (1973). Isolation of faster components in the electroretinogram and visually evoked response in man. *Am J Ophthalmol* 75: 846-852.

van Hof, M, & Usami, E (1967). The ERG in the newborn guinea pig. *Proceedings of the 6th ISCERG Symposium*, Erfurt, FRG: 291-295.

van Norren, D, and & Padmos, P (1975). The influence of various inhalation anesthetics on dark adaptation. *Doc Opthalmol* 11: 149-151.

Wachtmeister, L (1972). On the oscillatory potentials of the human electroretinogram in light and dark adaptation. *Acta Ophthalmol* (Copenh, Suppl): 116.

Wachtmeister, L (1973). On the oscillatory potentials ofthe human electroretinogram in light and dark adaptation. III- Thresholds and relation to stimulus intensity on adaptation to background light. *Acta Opthalmol* 51: 95-113.

Wachtmeister, L (1980). Further studies on the chemical sensitivity of the oscillatory potentials of the ERG: I gaba and glycine. *Acta Opthmol* S8: 712-725.

Wachtmeister, L, & Dowling, J (1978). The oscillatory potentials of the mudpuppy retina. *Invest Ophthalmol Vis Sci* 17: 1176-1188.

Wali, N, & Leguire, L (1992). The photopic hill: a new phenomenon of the light adaptation electroretinogram. *Doc Ophthalmol* 80: 335-342.

Winkelman, J, & Horsten, G (1962). The ERG of premature and full term born infants during their first days of life. *Ophthalmologica* 143: 92-101.

Xu, X, & Karwoski, CJ (1994). Current source density analysis of retinal field potentials: pharmacological analysis of the b-wave and M-wave. *J Neurophysiol.* 72: 96-102.

Xu, X, & Karwoski, CJ (1996). Rabbit ERG: Current source density (CSD) analysis (ARVO abstract). *Invest Ophthalmol Vis Sci* 37: S136.

Yanagida, T, Koshirnizu, M, Kawasaki, K, & Yonemura, D (1988). Micoelectrode depth study of the electroretinographic oscillatory potentials in the frog retina. *Doc Ophthalmol* 67: 355-361.

Yonemura, D, & Hatta, M (1966). Studies of the minor components of the frog's electroretinogram. *Jpn J Physiol* 16: 11-22.

Yonemura, D, Aoki, T, & Tsuzuki, K (1962). Electroretinogram in diabetic retinopathy. *Arch Ophthalmol* 68: 19-24.

Zetterström, B (1951). The clinical elelctroretinogram. IV. The electroretinogram in children during the first year of life. *Acta Opthalmol* 29: 295-304.